Uni-NaVid: A Video-based Vision-Language-Action Model for Unifying Embodied Navigation Tasks

Jiazhao Zhang 1,2 Kunyu Wang 2 Shaoan Wang 1,2 Minghan Li 2 Haoran Liu 1,2 Songlin Wei 1,2 Zhongyuan Wang 3 Zhizheng Zhang 2,3,† He Wang 1,2,3,† Peking University 2 Galbot 3 Beijing Academy of Artificial Intelligence

https://pku-epic.github.io/Uni-NaVid/

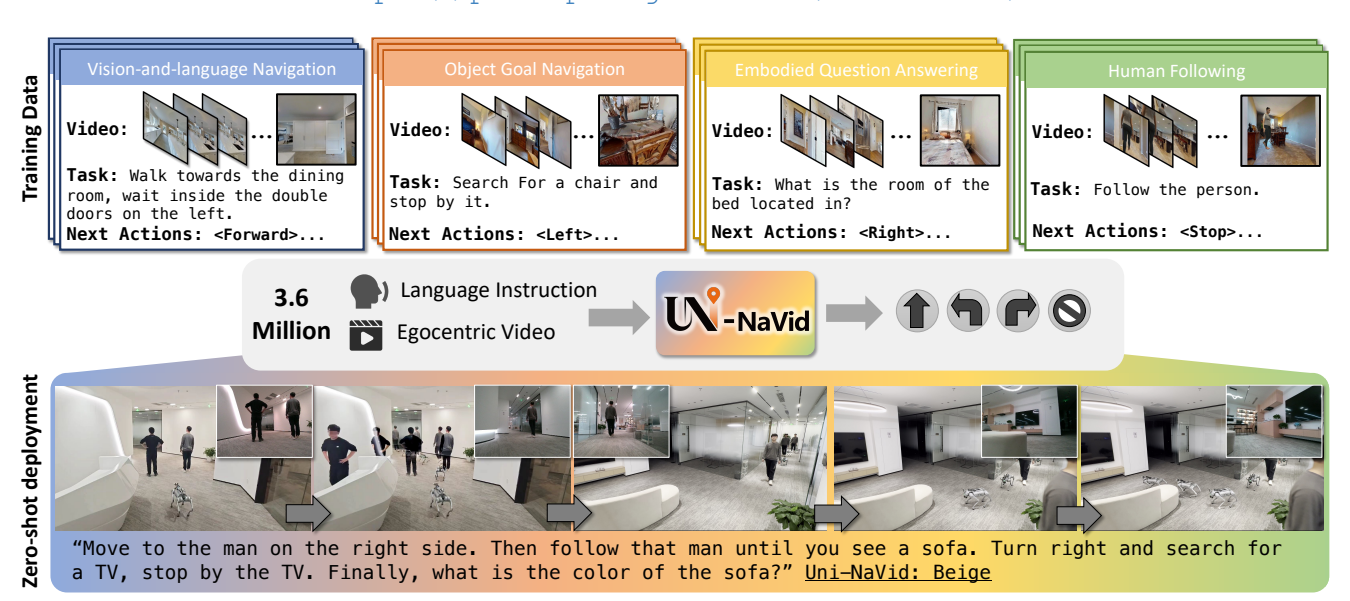


Figure 1. Uni-NaVid learns general navigation skills across four embodied navigation tasks using 3.6 million navigation samples. Uni-NaVid only takes online RGB video frames and language instructions as input and output actions, achieving general navigation ability in a real-world deployment.

Abstract

A practical navigation agent must be capable of handling a wide range of interaction demands, such as following instructions, searching objects, answering questions, tracking people, and more. Existing models for embodied navigation fall short of serving as practical generalists in the real world, as they are often constrained by specific task configurations or pre-defined maps with discretized waypoints. In this work, we present Uni-NaVid, the first video-based vision-language-action (VLA) model designed to unify diverse embodied navigation tasks and enable seamless navigation for mixed long-horizon tasks in unseen real-world environments. Uni-NaVid achieves this by harmonizing the input and output data configurations for all commonly used embodied navigation tasks and thereby integrating all tasks

First author (e-mail: zhngjizh@gmail.com). † Corresponding authors (e-mail: zhangzz@galbot.com, hewang@pku.edu.cn).

in one model. For training Uni-NaVid, we collect 3.6 million navigation data samples in total from four essential navigation sub-tasks and foster synergy in learning across them. Extensive experiments on comprehensive navigation benchmarks clearly demonstrate the advantages of unification modeling in Uni-NaVid and show it achieves state-of-the-art performance. Additionally, real-world experiments confirm the model's effectiveness and efficiency, shedding light on its strong generalizability.

1. Introduction

Embodied navigation is fundamental for supporting various interaction demands. Recently, instruction-following navigation techniques have advanced significantly with the development of multimodal models. However, existing studies [2, 51, 61, 66, 68, 79, 94, 96, 98, 100] either develop individual models for different tasks, *e.g.*, vision-and-

Methods	Act	Action Embodied Navigation Tasks						
Methods	D.E.	C.E.	VLN [37]	ObjNav [64]	EQA [18]	Follow [56]		
VLMaps [28]	V		✓	✓				
NaviLLM [98]	✓		✓	\checkmark	✓			
InstructNav [51]		\checkmark	✓	\checkmark				
Poliformer [90]		\checkmark		\checkmark		✓		
Uni-NaVid		\checkmark	✓	\checkmark	✓	✓		

Table 1. **Task and setting comparison.** Uni-NaVid is developed to address four embodied navigation tasks, generating action outputs in continuous environments. C.E.: Continuous Environment; D.E.: Discrete Environment.

language navigation [37, 39], object goal navigation [11], embodied question answering [18], following [30, 56, 97], *etc*, or explore task unification in a simplified setting (Tab. 1). They all fall short as full-stack navigation models qualified for practical general-purpose deployment.

Developing a full-stack navigation model poses significant challenges, not only in unifying task modeling but also in integrating heterogeneous data in joint use. Initial efforts adopt imitation learning (IL) [55, 72, 78] or reinforcement learning (RL) [82, 90] to learn general navigation skills in simulation environments or limited diverse real-world environments. However, due to the limited rendering quality and diversity of simulators, these approaches often encounter the "sim-to-real" gap and suffer from poor generalization across diverse navigation tasks [5, 22, 33]. Recent studies [50, 51, 67, 98, 100] have attempted to achieve a higher degree of unification on top of pre-trained LLMs, but they simplify the problem to some extent by adopting discretized modeling approaches. They rely on pre-defined graphs for learning decision-making, thus sacrificing the output flexibility and resulting in a low upper bound, especially for real-world deployment.

In this work, we build Uni-NaVid, a Vision-Language-Action (VLA) model for unifying diverse commonly demanded navigation tasks (Tab. 1). It takes video streams and natural language as input, adaptively generates actions following instructions, and automatically responds to questions if raised in an end-to-end manner. We make the first endeavor to address three essential questions, as elaborated below, in pursuit of ultimate real-world application.

How to unify different navigation tasks with minimal problem simplification and maximum utilization of data? We target an up-to-date unification modeling in Uni-NaVid where it takes single-view egocentric video streams and natural language as inputs, and end-to-end generate actions or linguistic responses for instructions or questions adaptively. We follow the natural characteristic of Large Language Models (LLMs) to cross-modally interleave the inputs and outputs of different navigation tasks into a single sequence in the token space to enable joint learning with next-token-prediction paradigm for Uni-NaVid. It incorporates four widely demanded navigation tasks, including Vision-and-Language Navigation (VLN), object-goal navigation, em-

bodied question answering, and human following. The corresponding training data are all collected from simulation environments. Besides, we further incorporate Internet realworld data for Video Question Answering (VQA) [7, 44] and video captioning [16] as auxiliary tasks into this unified model to enhance navigation performance and promote simto-real generalization. This is a groundbreaking attempt in this field at unified cross-modal, cross-task, and cross-simto-real modeling. It achieves impressive synergy in a broad range and results in a full-stack navigation agent.

How to improve the efficiency of such a unification design to enable a deployment-friendly model? In addition to unification modeling, we also prioritize efficient model design for practical deployment. Specifically, we adopt an online token merging mechanism to compress near historical frames with a relatively low ratio while compressing far historical frames with a relatively high ratio. In this way, Uni-NaVid learn compact representations that maintain not only fine-grained spatial information but also structured temporal information, thus speeding up the model inference by reducing the token number. Besides, Uni-NaVid adopts a foresight prediction to generate actions for a future horizon at once instead of step-by-step. This allows us to use an asynchronous strategy for action inference and execution.

How to verify the synergy between different tasks? We conduct comprehensive ablation studies to verify the synergy over different navigation tasks, as well as between simulation and real-world tasks in both simulation and real-world environments. We find they promote each other with unification modeling in such a broad range and help Uni-NaVid attain clear superiority in all sub-tasks [18, 31, 37, 64] compared to recent works. Besides, we also evaluate Uni-NaVid on long-horizon real-world tasks, which include multiple subtasks, and witness it can complete them in a zero-shot manner as shown in Figure 1.

By exploring these three essential questions, we demonstrate the advantages of unified modeling and joint data utilization across different tasks and in sim-to-real transfer. We hope this will foster future progress in developing an up-to-date full-stack navigation agent for general-purpose real-world applications.

2. Related Works

Generalist Embodied Navigation. Embodied navigation [2, 79, 96] requires agents to navigate in unseen environments based on human instructions. There is extensive literature on embodied navigation; here, we focus on four mainstream tasks that involve both visual information and language instructions: Vision-and-Language Navigation [4, 37, 39], Object Goal Navigation [11], Embodied Question Answering [18], and Human Following [31, 56]. Early efforts [55, 72, 78, 82] towards a generalist-embodied navigation model involved multi-task navigation datasets

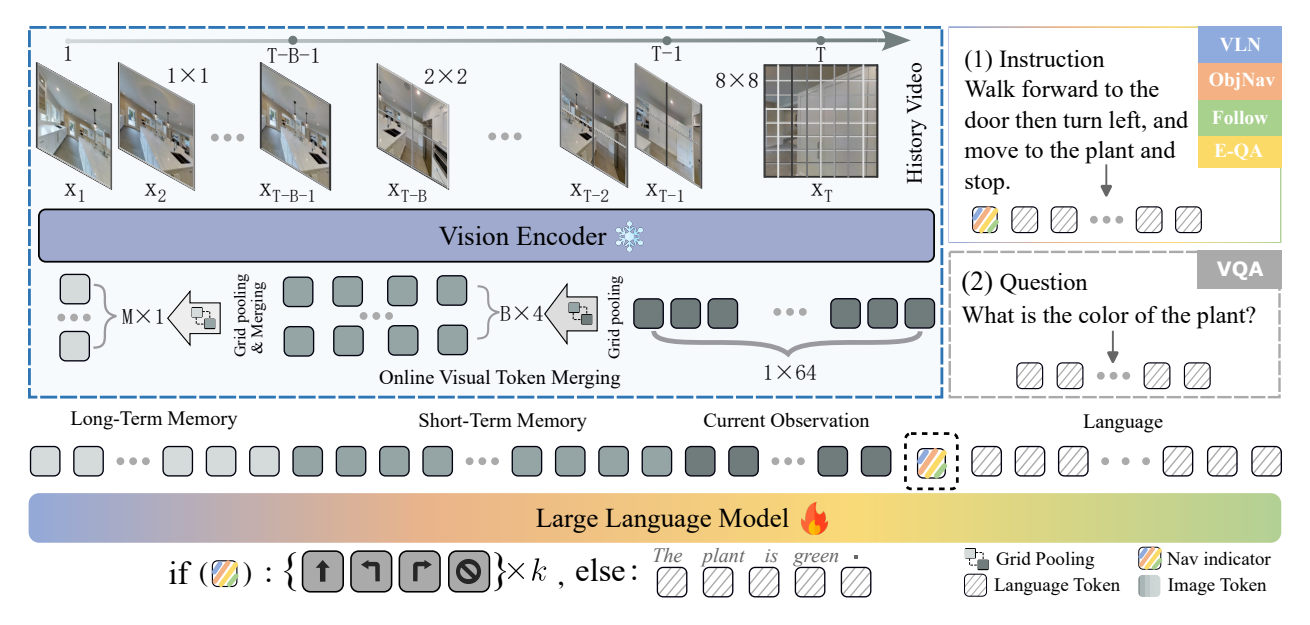


Figure 2. **Pipeline of Uni-NaVid.** Our method takes only single-view RGB frames $\{\mathbf{x}_1, \dots, \mathbf{x}_T\}$ and a natural language instruction \mathcal{I} as input. For each frame, we extract 64 visual tokens using the vision encoder and then use online token merging to accelerate the model while retaining compact visual information. The merged tokens and instruction tokens are sent to the large language model to obtain actions for navigation or answers for embodied question-answering.

and directly learning navigation skills, showing initial success in multi-task performance. However, these methods experienced performance drops when deployed in novel environments, especially in real-world settings. In recent years, advanced approaches [29, 50, 51, 67, 98, 101] have leveraged the generalization capabilities of large language models to improve multi-task navigation. These models show promising generalizability across navigation tasks but rely on extensive prompting, which impacts time efficiency. In contrast, our video-based large language model is trained end-to-end for multi-task navigation, offering robust generalization and computational efficiency for tasks like human following.

Large Language Models for Navigation. Large Language Models (LLMs)[17, 46, 102] have been introduced into robotic navigation due to their generalization capabilities in understanding and planning. One straightforward approach[50, 51, 67, 100] is to use off-the-shelf large language models in a zero-shot manner. These methods employ visual foundation models [19, 46] to describe surrounding environments in text format, prompting the language model to select landmarks that guide the agent. However, abstracting dense visual information into text and relying on discrete landmarks results in sparse environmental observations and is limited to static environments. Another approach [90, 95] trains a video-based large language model end-to-end with low-level actions to enable continuous movement. However, it faces efficiency challenges in long-horizon tasks. In contrast, Uni-NaVid implements an online visual token merging strategy, optimizing training efficiency for long-horizon tasks and supporting non-blocking execution in real-world environments.

3. Method

General navigation. We define the general navigation of Uni-NaVid as follows: At the time T, given a natural language instruction \mathcal{I} consisting of l words and an ego-centric RGB video \mathcal{O}_T comprising a sequence of frames $\{\mathbf{x}_1, \cdots, \mathbf{x}_T\}$, the agent is required to plan the next k actions $\{\mathcal{A}_T, \cdots, \mathcal{A}_{T+k-1}\}$ for it to complete the instruction within novel environments (k=4) in our experiments). Follow the most common settings [64], we adopts four low-level actions $\mathbf{a} \in \mathcal{A}$, including $\{\text{FORWARD}, \text{TURN-LEFT}, \text{TURN-RIGHT}, \text{STOP}\}$.

Overview. As shown in Figure 2, the architecture of Uni-NaVid is designed for general-purpose navigation which is composed of two main components: a vision encoder and a large language model (LLM). First, the video is encoded into a sequence of visual tokens via a vision encoder. The visual tokens are spatially and temporally merged, resulting in a compact sequence of visual tokens. Then they are projected into a space aligned with language tokens, which are referred to as observation tokens. As common, the instructions are also tokenized as a set of tokens, called instruction tokens. Both the observation and instruction tokens are concatenated and passed to the LLM, which infers 4 action tokens representing the next four actions.

3.1. Model of Uni-NaVid

Observation encoding. Given the ego-centric video up to time T, denoted by $\mathcal{O}_T = \{\mathbf{x}_1, \cdots, \mathbf{x}_T\}$, we encode the video to a sequence of observation tokens. For each frame \mathbf{x}_t , we first get its visual tokens $\mathbf{X}_t \in \mathbb{R}^{N_x \times C}$ with a vision encoder (EVA-CLIP [70] in implementation), where N_x is the patch number (N_x is set to 256) and C is the embedding dimension. Inspired by vision-language models [44, 46], we also perform a vision-language alignment by projecting the visual feature embedding into the language space, which denotes as observation tokens $\mathbf{E}_t^V \in \mathbb{R}^{N_x \times C}$.

$$\mathbf{E}_t^V = P_V(\mathbf{X}_t),\tag{1}$$

Where P_V represents the cross-modality projector. Although observation tokens provide crucial visual information for the agent to plan its next actions, the linearly increasing number of these tokens $(T \times N_x)$ leads to progressively longer processing times, making it impractical to use them directly for navigation purposes.

Online visual token merging. To balance the efficiency and effectiveness of visual tokens, we design a token merging strategy to retain navigation-relevant visual information for Uni-NaVid. This strategy builds on the key navigation insight that recent observations are more critical, and that visual information between consecutive frames and neighboring pixels could be redundant.

Drawing inspiration from the Atkinson-Shiffrin memory model [6, 69], we categorize visual tokens into current visual tokens \mathbf{X}_{curr} , short-term visual tokens \mathbf{X}_{short} , and longterm visual tokens X_{long} . These tokens are grouped based on their timestamps relative to the most recent frame. Current visual tokens capture sufficient visual information for the agent to perceive its immediate surroundings and to plan subsequent paths. Short-term visual tokens maintain temporal continuity, preserving relevant information momentarily to support ongoing planning. Long-term visual tokens facilitate the integration and retrieval of knowledge across the entire navigation history. For each category of visual tokens, we apply a grid pooling operation at different pooling resolutions:

$$\mathbf{X}_{1:T} = \begin{cases} \mathbf{X}_{\text{curr}} = GridPool(\mathbf{X}_t, \alpha_{\text{curr}}), & \text{if } \mathbf{t} = \mathbf{T} \\ \mathbf{X}_{\text{short}} = GridPool(\mathbf{X}_t, \alpha_{\text{short}}), & \text{if } \mathbf{t} \in [\text{T-B, T}) \\ \mathbf{X}_{\text{long}} = GridPool(\mathbf{X}_t, \alpha_{\text{long}}), & \text{if } \mathbf{t} \in [1, \text{T-B}) \end{cases}$$
(2)

where GridPool(·) is a grid pooling operation [44, 95], squeezing the tokens from N_x to $\frac{N_x}{\alpha^2}$, and B (set to 64) is the length of the buffer of shorter memory. Here, we adopt the $\alpha_{\mathrm{curr}}=2$, $\alpha_{\mathrm{short}}=8$, $\alpha_{\mathrm{long}}=16$, leads to visual tokens as $\mathbf{X}_{\mathrm{curr}}\in\mathbb{R}^{64\times C}$, $\mathbf{X}_{\mathrm{short}}\in\mathbb{R}^{4\times C}$, $\mathbf{X}_{\mathrm{long}}\in\mathbb{R}^{1\times C}$, respectively. These hyperparameters are determined through empirical experimentation and can be adjusted if memory and computational resources are not primary constraints.

In the navigation process, the agent consistently observes new frames. When a new frame at time T+1 arrives, we apply grid pooling to the most recent visual tokens at time Tand the oldest short-term visual tokens at time T - B, then insert them into the short-term and long-term visual tokens, respectively:

$$\mathbf{X}_{\text{curr}\to\text{short}} = GridPool(\mathbf{X}_{\text{curr}}, \frac{\alpha_{\text{short}}}{\alpha_{\text{curr}}}), \tag{3}$$

$$\mathbf{X}_{\text{short}\to\text{long}} = GridPool(\mathbf{X}_{\text{short}}, \frac{\alpha_{\text{long}}}{\alpha_{\text{short}}}). \tag{4}$$

$$\mathbf{X}_{\text{short}\to\text{long}} = GridPool(\mathbf{X}_{\text{short}}, \frac{\alpha_{\text{long}}}{\alpha_{\text{short}}}). \tag{4}$$

In this way, we can online update the short-term visual tokens and long-term visual tokens with previously generated tokens. Furthermore, we compare the cosine similarity of the $\mathbf{X}_{\text{short} \rightarrow \text{long}}$ with the latest long-term visual tokens X_{long} at time T - B - 1. If the similarity is above a given threshold τ , we merge them based on the number of frames previously merged in the latest long-term visual tokens, K.

$$\mathbf{X}_{\text{long}} = \frac{1}{K+1} \left(K \mathbf{X}_{\text{long}} + \mathbf{X}_{\text{short} \to \text{long}} \right),$$
 (5)

subject to
$$\cos(\mathbf{X}_{\text{long}}, \mathbf{X}_{\text{short} \to \text{long}}) > \tau.$$
 (6)

We insert new long-term visual tokens $\mathbf{X}_{\text{short} \rightarrow \text{long}}$ if their similarity falls below τ (empirically set to $\tau = 0.95$ [69]), which indicates they contain relatively distinct visual information. This fusion in temporal preserves the observation history in a highly compact form (in a length of $M \ll T - B - 1$), with minimal computational cost for merging these tokens. Only frames at the boundaries of the visual token types require computation through parallel pooling operations, making the process computationally efficient and naturally suited for online deployment in realworld navigation applications. Compared to existing videobased large language models [44, 69, 95], this merging strategy significantly reduces processing time, achieving an average of 0.2 seconds per inference. This improvement becomes increasingly notable when handling longer video sequences. A detailed analysis of time efficiency is provided in the Supplementary Materials.

Action planning. For action planning, we follow the existing work [95] and use special tokens <NAV> to inform the LLM to predict navigation actions. Accordingly, we concatenate the observation token sequence $\mathbf{E}_{1:T}^{V}$ (obtained through Eq. 1 with visual tokens of Eq. 2) with special token <NAV> and instruction tokens and input them into the LLM to infer 4 action tokens $\{\mathbf{E}_T^A, \cdots, \mathbf{E}_{T+3}^A\}$:

The action tokens belong to the discrete action set {FORWARD, TURN-LEFT, TURN-RIGHT, STOP}.

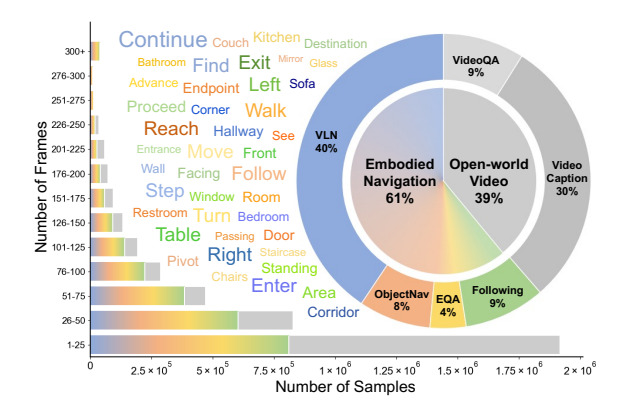


Figure 3. **Visualization of training data.** We visualize the combination of training data (5.9M), video frame counts, and the most common words in navigation instructions.

lowing the standard configuration in existing navigation settings [64, 90], the forward action corresponds to a movement of 25 cm, and the turning actions represent a 30° rotation. This configuration is consistent with all training navigation data (Sec. 3.2). Empirically, we find that predicting the next four steps yields optimal performance, which encourages Uni-NaVid to forecast long-horizon action sequences while still considering sufficient observations for accurate prediction. This multi-step prediction also supports asynchronous deployment, enabling non-blocking navigation performance in the real world. Please see the Supplementary Material for detailed elaboration.

3.2. Training of Uni-NaVid

To train a large-scale model for generalist navigation, it is essential to gather extensive and diverse navigation data across various tasks and environments. However, directly collecting vast amounts of real-world navigation data can be cost-prohibitive. To address this, we propose two key approaches for training Uni-NaVid: first, we collect multi-task navigation data in a wide range of synthetic environments (861 scenes in total), enabling Uni-NaVid to acquire general navigation skills; second, we co-tune Uni-NaVid with real-world video-based question-answering data, enhancing its understanding of real-world images and supporting its open-vocabulary knowledge.

Multi-task navigation data. We collect the largest multitask navigation dataset to date on the Habitat simulator environment [64], including 3.6M samples across four different navigation tasks introduced below. They are all curated in a unified format. Details are in Supplementary.

(A) Vision-and-language navigation [37] requires the agent to comprehend language instructions in order to follow the described path. We collect two types of instructions: one type uses landmarks and describes required motions between them, while the other specifies low-level actions, such as moving forward by 5 steps. We collect 2.4M

samples based on both VLN-CE R2R [37] and RxR [40].

- (B) Object goal navigation [64] involves the agent navigating an environment to locate a specific object based on provided visual or linguistic cues. This task assesses the agent's ability to perceive objects, understand spatial relationships, and execute efficient search strategies. We gather 483k samples from datasets on Habitat Matterport 3D dataset [57].
- (C) Embodied question answering [18] requires the agent to navigate to the related area for question answering. It involves spatial reasoning, object description, and understanding contextual information, requiring the ability to integrate perception, language comprehension, and decision-making. Following the setup in EQA [18], the agent first navigates to the target related to the question, issues a stop action, and then provides an answer. We collect 240k video-action samples and 10k video-answering samples on the EQA dataset [18] on Matterport 3D environments [10].
- (D) Human following [31] requires the agent to track and follow a human target with a specific description in dynamic and crowded environments, e.g., "Follow the man in the blue t-shirt.". The agent must recognize the appearance of the human, follow the correct person described in the instructions, predict their movement trajectory, and keep an appropriate distance while avoiding obstacles [20]. Based on the Habitat 3.0 social navigation environment [56], we collect 544k human-following navigation samples.

The data statistics can be found in Figure 3. Note that all data were collected from synthetic environments, including Habitat-Matterport and Matterport 3D, totaling 861 scenes. We use the default settings of each environment, with a height range from $0.88~\mathrm{m}$ to $1.25~\mathrm{m}$ and a robot radius between $0.1~\mathrm{m}$ and $0.6~\mathrm{m}$. This helps avoid overfitting to a specific robot embodiment.

Joint training on synthetic and real-world data. Although we collect navigation data from various environments, the diversity in both observations and instructions remains limited to a certain set of synthetic environments. To incorporate open-world knowledge, we follow previous VLA methods [8, 95], fine-tune Uni-NaVid using open-world video question-answering datasets. We collect 2.3M video question-answering data from publicly available datasets [7, 16, 44], leading to a total of 5.9M training samples. We adopt a two-stage training process: train the visual projector first, and then jointly train both the projector and the large language model. Further training details are provided in the Supplementary Materials.

3.3. Implementation Details

Training configuration. Uni-NaVid is trained on a cluster server with 40 NVIDIA H800 GPUs for approximately 35 hours, totaling 1400 GPU hours. For video data, we sample frames at 1 FPS to remove redundant information be-

tween consecutive frames. During training, EVA-CLIP [70] and Vicuna-7B [17] are pre-loaded with default pre-trained weight. Following the training strategy of VLM [46], we optimize the trainable parameters for only 1 epoch.

Benchmark evaluation and real-world deployment. For each navigation task, we adhere to its default settings [18, 31, 37, 64]. Specifically, for EQA [18], the agent executes actions based on the policy until a stop command is output. We then remove the navigation special token <NAV> and query the questions using the navigation history. For real-world deployment, we use a remote server with an NVIDIA A100 GPU to run Uni-NaVid, which processes observations (along with text instructions) and sends commands to a local robot to execute the predicted actions. Uni-NaVid requires approximately 0.2 seconds to generate the next four actions. During navigation, the robot asynchronously uploads the latest observations to the model while executing and pending future actions. Refer to the supplementary video for real-world navigation performance.

4. Experiment

We conduct experiments to evaluate Uni-NaVid on three specific aspects: (1) How does Uni-NaVid perform on individual tasks? (2) Does learning multiple navigation tasks lead to synergistic improvements? (3) Is the key design of our method effective? Due to space limitations, the complete set of protocols, additional results, and visualizations are provided in the Supplementary Materials.

Benchmarks. We evaluate our method on various benchmarks across different navigation tasks. For vision-and-language navigation tasks, we use Val-Unseen splits of R2R [37] and RxR [39] benchmarks. For object goal navigation, we use the validation split of Habitat Matterport 3D dataset [57]. For the embodied question-answering task, we use validation split of MP3D-EQA benchmark [18]. For the human following task, we leverage the Habitat 3.0 social navigation benchmark [56] and extend it to multiperson environments. For video understanding, we follow the evaluation manner of existing methods [44]. We choose ScanQA [7], MSVD [12], MSRVTT [81], and ActivityNet [9] for video question-answering evaluation.

Metrics. To evaluate navigation performance, we follow the standard evaluation metrics [4], including success rate (SR), oracle success rate (OS), success weighted by path length (SPL) [3], trajectory length (TL), following rate (FR) [56], collision rate (CR) [56] and navigation error from goal (NE). Note that the success criteria change among different navigation tasks, we therefore use the default success criteria of each benchmark. For video understanding evaluation, we employ widely used metrics following existing works [7, 44].

Method		Obse	rvation	1	VLN	-CE I	R2R V	Val-U	nseen
Method	Pan.	Odom.	Depth	S.RGB	TL	$NE\!\!\downarrow$	$\mathbf{OS} \uparrow$	$\mathbf{SR} \!\!\uparrow$	$\mathbf{SPL}\uparrow$
HPN+DN* [38]	V	✓	√		7.62	6.31	40.0	36.0	34.0
CMA* [25]	✓	\checkmark	\checkmark		10.90	6.20	52.0	41.0	36.0
VLN ♂BERT*† [25]	✓	\checkmark	\checkmark		12.23	5.74	53.0	44.0	39.0
Sim2Sim* [36]	✓	\checkmark	\checkmark		10.69	6.07	52.0	43.0	36.0
GridMM* [74]	✓	\checkmark	\checkmark		13.36	5.11	61.0	49.0	41.0
HAMT*‡ [73]	✓	\checkmark	\checkmark		-	4.80	_	55.0	51.0
ETPNav* [1]	✓	\checkmark	\checkmark		11.99	4.71	65.0	57.0	49.0
InstructNav [51]	√	√	√	√	7.74	6.89	-	31.0	24.0
AG-CMTP [13]	✓	\checkmark	\checkmark		-	7.90	39.2	23.1	19.1
R2R-CMTP [13]	✓	\checkmark	\checkmark		-	7.90	38.0	26.4	22.7
LAW [60]		\checkmark	\checkmark	\checkmark	8.89	6.83	44.0	35.0	31.0
CM2 [21]		\checkmark	\checkmark	\checkmark	11.54	7.02	41.5	34.3	27.6
WS-MGMap [14]		\checkmark	✓	✓	10.00	6.28	47.6	38.9	34.3
ETPNav.FF [75]		\checkmark	\checkmark	\checkmark	-	5.95	55.8	44.9	30.4
Seq2Seq [37]			✓	✓	9.30	7.77	37.0	25.0	22.0
CMA [37]			✓	✓	8.64	7.37	40.0	32.0	30.0
NaVid [95]				\checkmark	7.63	5.47	49.1	37.4	35.9
Uni-NaVid				\checkmark	9.71	5.58	53.3	47.0	42.7

Table 2. **Vision-and-language navigation (R2R).** Comparison on VLN-CE R2R [37] Val-Unseen. *: Methods use high-level action space. †: Methods use the same waypoint predictor proposed in [25]. ‡: Methods use additional visual data than MP3D scenes [10].

Method	O	bservati	on	VLN-CE RxR Val-Unseen				
Method	Odom.	Depth	S.RGB	TL	$NE\downarrow$	$\mathbf{OS} \!\!\uparrow$	$\textbf{SR} \!\!\uparrow$	$\mathbf{SPL}\uparrow$
LAW [60]	√	√	✓	4.01	10.87	21.0	8.0	8.0
CM2 [21]	✓	\checkmark	\checkmark	12.29	8.98	25.3	14.4	9.2
WS-MGMap* [14]	✓	\checkmark	\checkmark	10.80	9.83	29.8	15.0	12.1
ETPNav.FF [75]	✓	\checkmark	\checkmark	-	8.79	36.7	25.5	18.1
Seq2Seq* [37]		\checkmark	\checkmark	1.16	11.8	5.02	3.51	3.43
CMA* [37]		\checkmark	\checkmark	5.09	11.7	10.7	4.41	2.47
A^2 Nav † [15]			\checkmark	-	-	_	16.8	6.3
NaVid* [95]			\checkmark	10.59	8.41	34.5	23.8	21.2
Uni-NaVid			✓	15.8	6.24	55.5	48.7	40.9

Table 3. **Vision-and-language navigation (RxR).** Comparison on VLN-CE RxR [40] Val-Unseen. *: only trained on VLN-CE R2R.

4.1. Individual Task Results

Comparison on vision-and-language navigation. We evaluate our method with mainstream baselines on two publicly available benchmarks: VLN-CE R2R [37] and RxR [40]. The results are shown in Table 2 and Table 3. We find that our methods achieve SOTA-level performance on both datasets using only RGB videos as observations. In comparison to NaVid [95], which is also a vision language model that is solely trained on VLN data, our approach demonstrates significant improvements, with a $\pm 25.7\%$ increase in Success Rate (SR) on R2R. For zero-shot methods (InstructNav [51] and A²Nav [15]) that use ChatGPT with only text inputs for visual language navigation (VLN), these approaches often face challenges in transitioning between text prompts and visual information, resulting in less than satisfactory outcomes (almost half the SR of Uni-NaVid).

Comparison on object goal navigation. We conduct the experiments on HM3D [57] to compare Uni-NaVid with mainstream methods [58, 59, 77, 83, 84] that also learn from ObjectNav data. The results, shown in Table 4, demonstrate that our approach achieves the best performance. Note

Method	C	bservatio	HM3D ObjectNav		
Method	Odom.	Depth	S.RGB	SR↑	SPL↑
DD-PPO [77]	✓	✓	√	27.9	14.2
Habitat-Web [58]	✓	\checkmark	\checkmark	57.6	23.8
InstructNav [51]	✓	\checkmark	\checkmark	58.0	20.9
PIRLNav-IL [59]	✓		\checkmark	64.1	27.1
PIRLNav-IL-RL [59]	✓		\checkmark	70.4	34.1
OVRL [84]	✓		\checkmark	62.0	26.8
OVRL-v2 [83]	✓		\checkmark	64.7	28.1
Uni-NaVid			\checkmark	73.7	37.1

Table 4. **Object goal navigation.** Comparison on Habitat Matterport 3D [57] ObjectNav dataset.

Method	Action Type	MP3D EQA		
Method	D.E. C.E. GT	ACC↑		
NaviLLM [98]	✓	44.5		
Uni-NaVid	✓	47.3		
EQA(habitat-lab) [18]	✓	46.0		
NaviLLM [98]	✓	47.4		
Uni-NaVid	✓	54.4		

Table 5. **Embodied question answering.** Comparison on Habitat Matterport3D EQA dataset [18].

Method	Obser	vation	Human Following Dataset				
Method	H.Det.	S.RGB	SR↑	FR↑	CR↓		
PoliFormer [90]		√	2.79	20.35	2.93		
PoliFormer* [90]	✓	\checkmark	14.67	37.14	4.29		
PoliFormer† [90]	✓	\checkmark	25.29	47.16	6.78		
IBVS* [23]	✓	\checkmark	46.08	62.64	0.84		
IBVS† [23]	✓	\checkmark	50.58	68.89	0.80		
Uni-NaVid		\checkmark	61.21	71.93	2.07		

Table 6. **Human following.** Comparison on Human Following Dataset. *: Methods use GroundingDINO [49] as the open-vocabulary human detector. †: Methods use the ground-truth bounding box provided by the simulator.

that methods not utilizing odometry face challenges as they must rely on implicit memory to retain the historical trajectory. Nevertheless, Uni-NaVid still achieves significant gains in SR (+4.7%) and SPL (+8.8%) compared to previous state-of-the-art methods. Additionally, we believe our method's ObjectNav performance can be further enhanced by incorporating reinforcement learning techniques, as demonstrated by PIRLNav [59] and Poliformer [90].

Comparison on embodied question answering. The evaluation results on MP3D-EQA [18] are presented in Table 5. Despite navigating in continuous environments (CE), our method outperforms existing approaches (*e.g.*, NaviLLM [98] leverage the same evaluation strategy in Sec. 3.3) that operate within discrete landmark-based environments (DE). Moreover, when provided with the ground truth (GT) navigation trajectory, our method shows a significant improvement, demonstrating its ability to understand navigation history effectively.

Comparison on human following. We compared our method with two most relative methods PoliFormer [90] and IBVS [23]. Since both methods require a specific human bounding box as input, obtained from an upstream

Method	ScanQA								
Method	EM ↑	BLUE-1 \uparrow	$ROUGE \uparrow$	$METEOR \uparrow$	$CIDEr {\uparrow}$				
V.N.+MCAN [89]	19.71	29.46	30.97	12.07	58.23				
S.R.+MCAN [89]	20.56	27.85	30.68	11.97	57.56				
3D-LLM(flamingo) [26]	23.2	32.60	34.80	13.5	65.6				
NaviLLM [98]	26.27	39.73	40.23	16.56	80.77				
BridgeQA [54]	31.29	34.49	43.26	16.51	83.75				
Uni-NaVid	28.01	46.85	45.74	19.24	94.72				

Table 7. **Embodied video question answering.** Comparison on ScanQA [7] benchmark.

Method	MSV	D-QA	MSRV	/TT-QA	ActivityNet-QA		
Method	Acc↑	$Score \!\!\uparrow$	Acc↑	Score [↑]	Acc↑	Score [↑]	
VideoLLaMA [91]	51.6	2.5	29.6	1.8	12.4	1.1	
VideoChat [42]	56.3	2.8	45.0	2.5	26.5	2.2	
VideoChatGPT [52]	64.9	3.3	49.3	2.8	35.2	2.7	
BT-Adapter [47]	67.5	3.7	57.0	3.2	45.7	3.2	
Chat-UniVi [32]	65.0	3.6	54.6	3.1	45.8	3.2	
LLaMA-VID [44]	69.7	3.7	57.7	3.2	47.4	3.3	
VideoChat2 [43]	70.0	3.9	54.1	3.3	49.1	3.3	
Video-LLaVA [45]	70.7	3.9	59.2	3.5	45.3	3.3	
ST-LLM [48]	74.6	3.9	63.2	3.4	50.9	3.3	
Uni-NaVid	69.6	3.9	59.3	3.5	51.4	3.7	

Table 8. **Video question answering.** Comparison with leading methods (all based on Vicuna-7B [17]) on VQA benchamarks.

algorithm, we use the bounding box from the open-world object detector GroundingDINO [49] and the ground truth provided by the simulator to evaluate the human following performance of the comparison methods under various setups. As shown in Table 6, Uni-NaVid outperforms the comparison methods on both SR (+21.0%) and FR (+4.4%) while maintaining low CR under any setup, even when they use ground truth bounding boxes as input. This demonstrates that Uni-NaVid can effectively infer instructions and follow the correct human, as well as predict the human's movement patterns accurately.

Comparison on video question answering. We first evaluate our method on ScanQA [7] on Tab. 7. Compared to mainstream baselines, we find that Uni-NaVid archives the best performance on four metrics, including BLUE-1 (+17.9%), ROUGE (+5.7%), METEOR (+16.2%), and CIDEr (+13.1%). This proves the superiority of our methods on spatial scene understanding. Note that the EM metric requires an exact match between the question and answer, which is not well-suited to our method, as it is designed to learn from diverse data and generate flexible responses. We also compare our method on open-ended video question answering benchmark in Tab. 8, where we show comparable performance to SOTA methods.

4.2. Qualitative Results in Real-World

Figure 4 visualizes the results of all tasks in real-world environments. Despite training only on synthetic data, Uni-NaVid demonstrates impressive adaptability across various real-world settings, successfully performing multi-task nav-



Figure 4. Visual results of Uni-NaVid in real-world. We deploy Uni-NaVid across diverse environments to execute instructions in a zero-shot setting. We provide both third-person views and the robot's trajectory, showing effective multi-task navigation performance.

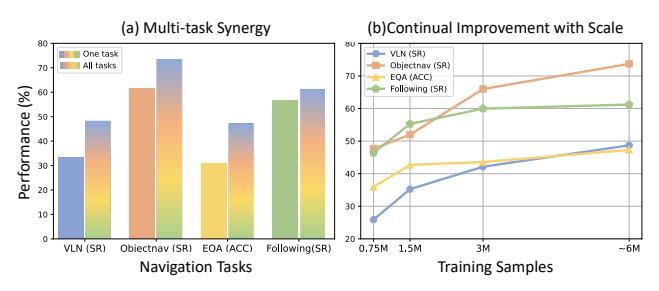


Figure 5. Comparsion on data scale and multi-task training.

igation. It effectively aligns navigation history with given instructions, identifies novel objects outside the training set, and avoids obstacles in densely populated areas. Additionally, it reliably follows human movement across diverse environments. Supplementary materials provide numerical results and further visualizations of challenging scenarios.

4.3. Ablation Study

We present a visualization of the training strategy's performance in Figure 5. This comparison contrasts training on a single navigation task with training across multiple tasks. The results (Figure 5 (a)) illustrate the synergistic benefits of multi-task learning, yielding consistent performance gains across all navigation tasks. Notably, VLN, ObjectNav, and EQA exhibit more substantial improvements, while Following shows comparatively smaller gains. We attribute this to the lower dependence of the following task on historical context. Additionally, we investigate the influence of data scale on performance (Figure 5 (b)), observing that performance improves across all navigation tasks with larger data volumes. However, the incremental gain diminishes (from 3M to 6M samples), potentially due to limitations in the data diversity of simulators.

We conduct experiments to evaluate the effectiveness of the training strategy and visual token designs (Tab. 9). Our

Design	VLN (SR↑)	ObjNav (SR↑)	EQA (ACC↑)	Follow (SR↑)
No <nav> token</nav>	35.2	69.1	20.4	55.1
No VQA data	40.5	50.6	1.19	58.8
Curr.	9.61	44.3	32.5	56.3
Curr.+Short.	39.7	67.8	44.1	59.7
Curr.+Short.+Long.	48.7	73.7	47.3	61.2

Table 9. Ablation study on both training strategy and architecture.

results indicate that the absence of <NAV> and VQA data leads to a performance decline across all tasks. Notably, the performance drop is most pronounced in EQA, as the lack of <NAV> special token makes the model misinterpret whether it should answer questions or output actions. Additionally, without VQA data, the agent's ability to answer questions using visual information is greatly impaired.

From the performance of different memory designs, we find that both short-term and long-term memory visual tokens contribute to performance improvements. In particular, the VLN task shows the most significant performance drop (-80.3% SR) when visual memory is removed, as the lack of memory hinders the alignment of visual history with instructions. For the Following task, the absence of memory results in only a minor performance decline (-8% SR), as this task primarily relies on recent frames to track the target. Additional ablation studies are provided in the Supplementary Material.

5. Conclusion

We introduce a vision-language-action model, Uni-NaVid, designed to acquire general embodied navigation skills through multi-task navigation data. To efficiently encode the extended video sequences encountered in navigation, we develop an online visual token merging strategy that separately processes current observations, short-term observations, and long-term observations. This design allows our approach to operate at an average speed of 5 Hz. Exten-

sive experiments across publicly available benchmarks reveal our model's superior performance. The ablation studies demonstrate the synergy achieved by learning across multiple navigation tasks and prove the effectiveness of our key designs. In the future, we will explore the synergy between more fundamental embodied skills, integrating both manipulation and navigation.

References

- [1] Dong An, Hanqing Wang, Wenguan Wang, Zun Wang, Yan Huang, Keji He, and Liang Wang. Etpnav: Evolving topological planning for vision-language navigation in continuous environments. arXiv preprint arXiv:2304.03047, 2023.
- [2] Peter Anderson, Angel Chang, Devendra Singh Chaplot, Alexey Dosovitskiy, Saurabh Gupta, Vladlen Koltun, Jana Kosecka, Jitendra Malik, Roozbeh Mottaghi, Manolis Savva, et al. On evaluation of embodied navigation agents. *arXiv preprint arXiv:1807.06757*, 2018. 1, 2
- [3] Peter Anderson, Angel Chang, Devendra Singh Chaplot, Alexey Dosovitskiy, Saurabh Gupta, Vladlen Koltun, Jana Kosecka, Jitendra Malik, Roozbeh Mottaghi, Manolis Savva, et al. On evaluation of embodied navigation agents. arXiv preprint arXiv:1807.06757, 2018. 6
- [4] Peter Anderson, Qi Wu, Damien Teney, Jake Bruce, Mark Johnson, Niko Sünderhauf, Ian Reid, Stephen Gould, and Anton Van Den Hengel. Vision-and-language navigation: Interpreting visually-grounded navigation instructions in real environments. In Proceedings of the IEEE conference on computer vision and pattern recognition, pages 3674– 3683, 2018. 2, 6
- [5] Peter Anderson, Ayush Shrivastava, Joanne Truong, Arjun Majumdar, Devi Parikh, Dhruv Batra, and Stefan Lee. Simto-real transfer for vision-and-language navigation. In *Con*ference on Robot Learning, pages 671–681. PMLR, 2021.
- [6] RC Atkinson and RM Shiffrin. Human memory: A proposed system and its control processes (vol. 2). The Psychology of Learning and Motivation: Advances in Research and Theory, pages 89–195, 1968. 4
- [7] Daichi Azuma, Taiki Miyanishi, Shuhei Kurita, and Motoaki Kawanabe. Scanqa: 3d question answering for spatial scene understanding. In proceedings of the IEEE/CVF conference on computer vision and pattern recognition, pages 19129–19139, 2022. 2, 5, 6, 7, 18
- [8] Anthony Brohan, Noah Brown, Justice Carbajal, Yevgen Chebotar, Xi Chen, Krzysztof Choromanski, Tianli Ding, Danny Driess, Avinava Dubey, Chelsea Finn, et al. Rt-2: Vision-language-action models transfer web knowledge to robotic control. arXiv preprint arXiv:2307.15818, 2023. 5
- [9] Fabian Caba Heilbron, Victor Escorcia, Bernard Ghanem, and Juan Carlos Niebles. Activitynet: A large-scale video benchmark for human activity understanding. In *Proceedings of the ieee conference on computer vision and pattern recognition*, pages 961–970, 2015. 6
- [10] Angel Chang, Angela Dai, Thomas Funkhouser, Maciej Halber, Matthias Niebner, Manolis Savva, Shuran Song,

- Andy Zeng, and Yinda Zhang. Matterport3d: Learning from rgb-d data in indoor environments. In 2017 International Conference on 3D Vision (3DV), pages 667–676. IEEE, 2017. 5, 6, 19
- [11] Devendra Singh Chaplot, Dhiraj Prakashchand Gandhi, Abhinav Gupta, and Russ R Salakhutdinov. Object goal navigation using goal-oriented semantic exploration. *Advances in Neural Information Processing Systems*, 33:4247–4258, 2020. 2
- [12] David Chen and William B Dolan. Collecting highly parallel data for paraphrase evaluation. In *Proceedings of the 49th annual meeting of the association for computational linguistics: human language technologies*, pages 190–200, 2011. 6
- [13] Kevin Chen, Junshen K Chen, Jo Chuang, Marynel Vázquez, and Silvio Savarese. Topological planning with transformers for vision-and-language navigation. In Proceedings of the IEEE/CVF Conference on Computer Vision and Pattern Recognition, pages 11276–11286, 2021. 6
- [14] Peihao Chen, Dongyu Ji, Kunyang Lin, Runhao Zeng, Thomas H Li, Mingkui Tan, and Chuang Gan. Weakly-supervised multi-granularity map learning for vision-and-language navigation. *arXiv preprint arXiv:2210.07506*, 2022. 6, 19
- [15] Peihao Chen, Xinyu Sun, Hongyan Zhi, Runhao Zeng, Thomas H Li, Gaowen Liu, Mingkui Tan, and Chuang Gan. Action-aware zero-shot robot navigation by exploiting vision-and-language ability of foundation models. arXiv preprint arXiv:2308.07997, 2023. 6, 19
- [16] Tsai-Shien Chen, Aliaksandr Siarohin, Willi Menapace, Ekaterina Deyneka, Hsiang-wei Chao, Byung Eun Jeon, Yuwei Fang, Hsin-Ying Lee, Jian Ren, Ming-Hsuan Yang, et al. Panda-70m: Captioning 70m videos with multiple cross-modality teachers. In *Proceedings of the IEEE/CVF* Conference on Computer Vision and Pattern Recognition, pages 13320–13331, 2024. 2, 5, 16
- [17] Wei-Lin Chiang, Zhuohan Li, Zi Lin, Ying Sheng, Zhanghao Wu, Hao Zhang, Lianmin Zheng, Siyuan Zhuang, Yonghao Zhuang, Joseph E Gonzalez, et al. Vicuna: An open-source chatbot impressing gpt-4 with 90%* chatgpt quality. See https://vicuna. lmsys. org (accessed 14 April 2023), 2023. 3, 6, 7
- [18] Abhishek Das, Samyak Datta, Georgia Gkioxari, Stefan Lee, Devi Parikh, and Dhruv Batra. Embodied question answering. In *Proceedings of the IEEE conference on computer vision and pattern recognition*, pages 1–10, 2018. 2, 5, 6, 7, 14, 16
- [19] Vishnu Sashank Dorbala, Gunnar Sigurdsson, Robinson Piramuthu, Jesse Thomason, and Gaurav S Sukhatme. Clipnav: Using clip for zero-shot vision-and-language navigation. *arXiv preprint arXiv:2211.16649*, 2022. 3
- [20] Anthony Francis, Claudia Pérez-d'Arpino, Chengshu Li, Fei Xia, Alexandre Alahi, Rachid Alami, Aniket Bera, Abhijat Biswas, Joydeep Biswas, Rohan Chandra, et al. Principles and guidelines for evaluating social robot navigation algorithms. arXiv preprint arXiv:2306.16740, 2023. 5
- [21] Georgios Georgakis, Karl Schmeckpeper, Karan Wanchoo, Soham Dan, Eleni Miltsakaki, Dan Roth, and Kostas Dani-

- ilidis. Cross-modal map learning for vision and language navigation. In *Proceedings of the IEEE/CVF Conference on Computer Vision and Pattern Recognition*, pages 15460–15470, 2022. 6, 19
- [22] Theophile Gervet, Soumith Chintala, Dhruv Batra, Jitendra Malik, and Devendra Singh Chaplot. Navigating to objects in the real world. *Science Robotics*, 8(79):eadf6991, 2023.
- [23] Meenakshi Gupta, Swagat Kumar, Laxmidhar Behera, and Venkatesh K Subramanian. A novel vision-based tracking algorithm for a human-following mobile robot. *IEEE Transactions on Systems, Man, and Cybernetics: Systems*, 47(7):1415–1427, 2016. 7, 15, 20
- [24] Wenyi Hong, Weihan Wang, Ming Ding, Wenmeng Yu, Qingsong Lv, Yan Wang, Yean Cheng, Shiyu Huang, Junhui Ji, Zhao Xue, Lei Zhao, Zhuoyi Yang, Xiaotao Gu, Xiaohan Zhang, Guanyu Feng, Da Yin, Zihan Wang, Ji Qi, Xixuan Song, Peng Zhang, De-Feng Liu, Bin Xu, Juanzi Li, Yu-Chen Dong, and Jie Tang. Cogvlm2: Visual language models for image and video understanding. *ArXiv*, abs/2408.16500, 2024. 15
- [25] Yicong Hong, Zun Wang, Qi Wu, and Stephen Gould. Bridging the gap between learning in discrete and continuous environments for vision-and-language navigation. In Proceedings of the IEEE/CVF Conference on Computer Vision and Pattern Recognition, pages 15439–15449, 2022.
- [26] Yining Hong, Haoyu Zhen, Peihao Chen, Shuhong Zheng, Yilun Du, Zhenfang Chen, and Chuang Gan. 3d-llm: Injecting the 3d world into large language models. *Advances in Neural Information Processing Systems*, 36:20482–20494, 2023. 7
- [27] Shanee S Honig, Tal Oron-Gilad, Hanan Zaichyk, Vardit Sarne-Fleischmann, Samuel Olatunji, and Yael Edan. Toward socially aware person-following robots. *IEEE Trans*actions on Cognitive and Developmental Systems, 10(4): 936–954, 2018. 15
- [28] Chenguang Huang, Oier Mees, Andy Zeng, and Wolfram Burgard. Visual language maps for robot navigation. *arXiv* preprint arXiv:2210.05714, 2022. 2
- [29] Chenguang Huang, Oier Mees, Andy Zeng, and Wolfram Burgard. Visual language maps for robot navigation. In 2023 IEEE International Conference on Robotics and Automation (ICRA), pages 10608–10615. IEEE, 2023. 3
- [30] Yulong Huang, Yonggang Zhang, Peng Shi, Zhemin Wu, Junhui Qian, and Jonathon A Chambers. Robust kalman filters based on gaussian scale mixture distributions with application to target tracking. *IEEE Transactions on Systems, Man, and Cybernetics: Systems*, 49(10):2082–2096, 2017. 2
- [31] Md Jahidul Islam, Jungseok Hong, and Junaed Sattar. Person-following by autonomous robots: A categorical overview. *The International Journal of Robotics Research*, 38(14):1581–1618, 2019. 2, 5, 6, 15
- [32] Peng Jin, Ryuichi Takanobu, Wancai Zhang, Xiaochun Cao, and Li Yuan. Chat-univi: Unified visual representation empowers large language models with image and video understanding. In *Proceedings of the IEEE/CVF Conference on*

- Computer Vision and Pattern Recognition, pages 13700–13710, 2024. 7
- [33] Abhishek Kadian, Joanne Truong, Aaron Gokaslan, Alexander Clegg, Erik Wijmans, Stefan Lee, Manolis Savva, Sonia Chernova, and Dhruv Batra. Sim2real predictivity: Does evaluation in simulation predict real-world performance? *IEEE Robotics and Automation Letters*, 5 (4):6670–6677, 2020. 2
- [34] Linh Kästner, Bassel Fatloun, Zhengcheng Shen, Daniel Gawrisch, and Jens Lambrecht. Human-following and-guiding in crowded environments using semantic deep-reinforcement-learning for mobile service robots. In 2022 International Conference on Robotics and Automation (ICRA), pages 833–839. IEEE, 2022. 15
- [35] Mukul Khanna, Yongsen Mao, Hanxiao Jiang, Sanjay Haresh, Brennan Shacklett, Dhruv Batra, Alexander Clegg, Eric Undersander, Angel X Chang, and Manolis Savva. Habitat synthetic scenes dataset (hssd-200): An analysis of 3d scene scale and realism tradeoffs for objectgoal navigation. In Proceedings of the IEEE/CVF Conference on Computer Vision and Pattern Recognition, pages 16384–16393, 2024. 19
- [36] Jacob Krantz and Stefan Lee. Sim-2-sim transfer for visionand-language navigation in continuous environments. In European Conference on Computer Vision, pages 588–603. Springer, 2022. 6
- [37] Jacob Krantz, Erik Wijmans, Arjun Majumdar, Dhruv Batra, and Stefan Lee. Beyond the nav-graph: Vision-and-language navigation in continuous environments. In European Conference on Computer Vision, 2020. 2, 5, 6, 14, 16, 18, 19
- [38] Jacob Krantz, Aaron Gokaslan, Dhruv Batra, Stefan Lee, and Oleksandr Maksymets. Waypoint models for instruction-guided navigation in continuous environments. In Proceedings of the IEEE/CVF International Conference on Computer Vision, pages 15162–15171, 2021. 6
- [39] Alexander Ku, Peter Anderson, Roma Patel, Eugene Ie, and Jason Baldridge. Room-across-room: Multilingual vision-and-language navigation with dense spatiotemporal grounding. In *Proceedings of the 2020 Conference on Empirical Methods in Natural Language Processing (EMNLP)*, pages 4392–4412, 2020. 2, 6, 16
- [40] Alexander Ku, Peter Anderson, Roma Patel, Eugene Ie, and Jason Baldridge. Room-across-room: Multilingual vision-and-language navigation with dense spatiotemporal grounding. In *Proceedings of the 2020 Conference on Empirical Methods in Natural Language Processing (EMNLP)*, pages 4392–4412, 2020. 5, 6, 14, 19
- [41] Yuxuan Kuang, Hai Lin, and Meng Jiang. Openfmnav: Towards open-set zero-shot object navigation via vision-language foundation models. arXiv preprint arXiv:2402.10670, 2024. 17
- [42] KunChang Li, Yinan He, Yi Wang, Yizhuo Li, Wenhai Wang, Ping Luo, Yali Wang, Limin Wang, and Yu Qiao. Videochat: Chat-centric video understanding. arXiv preprint arXiv:2305.06355, 2023. 7
- [43] Kunchang Li, Yali Wang, Yinan He, Yizhuo Li, Yi Wang, Yi Liu, Zun Wang, Jilan Xu, Guo Chen, Ping Luo, et al.

- Mvbench: A comprehensive multi-modal video understanding benchmark. In *Proceedings of the IEEE/CVF Conference on Computer Vision and Pattern Recognition*, pages 22195–22206, 2024. 7
- [44] Yanwei Li, Chengyao Wang, and Jiaya Jia. Llama-vid: An image is worth 2 tokens in large language models. *arXiv* preprint arXiv:2311.17043, 2023. 2, 4, 5, 6, 7, 16, 20
- [45] Bin Lin, Yang Ye, Bin Zhu, Jiaxi Cui, Munan Ning, Peng Jin, and Li Yuan. Video-llava: Learning united visual representation by alignment before projection. arXiv preprint arXiv:2311.10122, 2023. 7
- [46] Haotian Liu, Chunyuan Li, Qingyang Wu, and Yong Jae Lee. Visual instruction tuning. In *NeurIPS*, 2023. 3, 4, 6
- [47] Ruyang Liu, Chen Li, Yixiao Ge, Thomas H Li, Ying Shan, and Ge Li. Bt-adapter: Video conversation is feasible without video instruction tuning. In *Proceedings of the IEEE/CVF Conference on Computer Vision and Pattern Recognition*, pages 13658–13667, 2024. 7
- [48] Ruyang Liu, Chen Li, Haoran Tang, Yixiao Ge, Ying Shan, and Ge Li. St-llm: Large language models are effective temporal learners. In *European Conference on Computer Vision*, pages 1–18. Springer, 2025. 7, 15
- [49] Shilong Liu, Zhaoyang Zeng, Tianhe Ren, Feng Li, Hao Zhang, Jie Yang, Qing Jiang, Chunyuan Li, Jianwei Yang, Hang Su, et al. Grounding dino: Marrying dino with grounded pre-training for open-set object detection. arXiv preprint arXiv:2303.05499, 2023. 7, 20
- [50] Yuxing Long, Xiaoqi Li, Wenzhe Cai, and Hao Dong. Discuss before moving: Visual language navigation via multi-expert discussions. arXiv preprint arXiv:2309.11382, 2023.
 2, 3
- [51] Yuxing Long, Wenzhe Cai, Hongcheng Wang, Guanqi Zhan, and Hao Dong. Instructnav: Zero-shot system for generic instruction navigation in unexplored environment. arXiv preprint arXiv:2406.04882, 2024. 1, 2, 3, 6, 7, 14
- [52] Muhammad Maaz, Hanoona Rasheed, Salman Khan, and Fahad Shahbaz Khan. Video-chatgpt: Towards detailed video understanding via large vision and language models. arXiv preprint arXiv:2306.05424, 2023. 7
- [53] Arjun Majumdar, Anurag Ajay, Xiaohan Zhang, Pranav Putta, Sriram Yenamandra, Mikael Henaff, Sneha Silwal, Paul Mcvay, Oleksandr Maksymets, Sergio Arnaud, et al. Openeqa: Embodied question answering in the era of foundation models. In Proceedings of the IEEE/CVF Conference on Computer Vision and Pattern Recognition, pages 16488–16498, 2024. 18, 19
- [54] Wentao Mo and Yang Liu. Bridging the gap between 2d and 3d visual question answering: A fusion approach for 3d vqa. In *Proceedings of the AAAI Conference on Artificial Intelligence*, pages 4261–4268, 2024. 7
- [55] Khanh Nguyen, Debadeepta Dey, Chris Brockett, and Bill Dolan. Vision-based navigation with language-based assistance via imitation learning with indirect intervention. In Proceedings of the IEEE/CVF Conference on Computer Vision and Pattern Recognition, pages 12527–12537, 2019.
- [56] Xavier Puig, Eric Undersander, Andrew Szot, Mikael Dallaire Cote, Tsung-Yen Yang, Ruslan Partsey, Ruta Desai,

- Alexander William Clegg, Michal Hlavac, So Yeon Min, et al. Habitat 3.0: A co-habitat for humans, avatars and robots. *arXiv preprint arXiv:2310.13724*, 2023. 2, 5, 6, 15
- [57] Santhosh Kumar Ramakrishnan, Aaron Gokaslan, Erik Wijmans, Oleksandr Maksymets, Alexander Clegg, John M Turner, Eric Undersander, Wojciech Galuba, Andrew Westbury, Angel X Chang, et al. Habitat-matterport 3d dataset (hm3d): 1000 large-scale 3d environments for embodied ai. In Thirty-fifth Conference on Neural Information Processing Systems Datasets and Benchmarks Track (Round 2), 2021. 5, 6, 7, 16
- [58] Ram Ramrakhya, Eric Undersander, Dhruv Batra, and Abhishek Das. Habitat-web: Learning embodied object-search strategies from human demonstrations at scale. In *Proceedings of the IEEE/CVF Conference on Computer Vision and Pattern Recognition*, pages 5173–5183, 2022. 6, 7
- [59] Ram Ramrakhya, Dhruv Batra, Erik Wijmans, and Abhishek Das. Pirlnav: Pretraining with imitation and rl fine-tuning for objectnav. In *Proceedings of the IEEE/CVF Conference on Computer Vision and Pattern Recognition*, pages 17896–17906, 2023. 6, 7
- [60] Sonia Raychaudhuri, Saim Wani, Shivansh Patel, Unnat Jain, and Angel X Chang. Language-aligned way-point (law) supervision for vision-and-language navigation in continuous environments. arXiv preprint arXiv:2109.15207, 2021. 6, 19
- [61] Nicole Robinson, Brendan Tidd, Dylan Campbell, Dana Kulić, and Peter Corke. Robotic vision for human-robot interaction and collaboration: A survey and systematic review. ACM Transactions on Human-Robot Interaction, 12 (1):1–66, 2023. 1
- [62] Stéphane Ross, Geoffrey Gordon, and Drew Bagnell. A reduction of imitation learning and structured prediction to no-regret online learning. In *Proceedings of the four*teenth international conference on artificial intelligence and statistics, pages 627–635. JMLR Workshop and Conference Proceedings, 2011. 16
- [63] Manolis Savva, Abhishek Kadian, Oleksandr Maksymets, Yili Zhao, Erik Wijmans, Bhavana Jain, Julian Straub, Jia Liu, Vladlen Koltun, Jitendra Malik, Devi Parikh, and Dhruv Batra. Habitat: A Platform for Embodied AI Research. ICCV, 2019. 16
- [64] Manolis Savva, Abhishek Kadian, Oleksandr Maksymets, Yili Zhao, Erik Wijmans, Bhavana Jain, Julian Straub, Jia Liu, Vladlen Koltun, Jitendra Malik, et al. Habitat: A platform for embodied ai research. In *Proceedings of the IEEE/CVF International Conference on Computer Vision*, pages 9339–9347, 2019. 2, 3, 5, 6, 14, 17, 18
- [65] James A Sethian. Fast marching methods. SIAM review, 41 (2):199–235, 1999. 16
- [66] Dhruv Shah, Michael Robert Equi, Błażej Osiński, Fei Xia, Brian Ichter, and Sergey Levine. Navigation with large language models: Semantic guesswork as a heuristic for planning. In *Conference on Robot Learning*, pages 2683–2699. PMLR, 2023.
- [67] Dhruv Shah, Błażej Osiński, Sergey Levine, et al. Lmnav: Robotic navigation with large pre-trained models of

- language, vision, and action. In *Conference on robot learning*, pages 492–504. PMLR, 2023. 2, 3
- [68] Dhruv Shah, Ajay Sridhar, Arjun Bhorkar, Noriaki Hirose, and Sergey Levine. Gnm: A general navigation model to drive any robot. In 2023 IEEE International Conference on Robotics and Automation (ICRA), pages 7226–7233. IEEE, 2023. 1
- [69] Enxin Song, Wenhao Chai, Guanhong Wang, Yucheng Zhang, Haoyang Zhou, Feiyang Wu, Haozhe Chi, Xun Guo, Tian Ye, Yanting Zhang, et al. Moviechat: From dense token to sparse memory for long video understanding. In Proceedings of the IEEE/CVF Conference on Computer Vision and Pattern Recognition, pages 18221–18232, 2024. 4, 15
- [70] Quan Sun, Yuxin Fang, Ledell Wu, Xinlong Wang, and Yue Cao. Eva-clip: Improved training techniques for clip at scale. arXiv preprint arXiv:2303.15389, 2023. 4, 6
- [71] Nguyen Van Toan, Minh Do Hoang, Phan Bui Khoi, and Soo-Yeong Yi. The human-following strategy for mobile robots in mixed environments. *Robotics and Autonomous Systems*, 160:104317, 2023. 15
- [72] Hanqing Wang, Wei Liang, Luc V Gool, and Wenguan Wang. Towards versatile embodied navigation. Advances in neural information processing systems, 35:36858–36874, 2022. 2
- [73] Zun Wang, Jialu Li, Yicong Hong, Yi Wang, Qi Wu, Mohit Bansal, Stephen Gould, Hao Tan, and Yu Qiao. Scaling data generation in vision-and-language navigation. In Proceedings of the IEEE/CVF International Conference on Computer Vision, pages 12009–12020, 2023. 6
- [74] Zihan Wang, Xiangyang Li, Jiahao Yang, Yeqi Liu, and Shuqiang Jiang. Gridmm: Grid memory map for vision-and-language navigation. In *Proceedings of the IEEE/CVF International Conference on Computer Vision*, pages 15625–15636, 2023. 6
- [75] Zihan Wang, Xiangyang Li, Jiahao Yang, Yeqi Liu, and Shuqiang Jiang. Sim-to-real transfer via 3d feature fields for vision-and-language navigation. arXiv preprint arXiv:2406.09798, 2024. 6, 19
- [76] Erik Wijmans, Samyak Datta, Oleksandr Maksymets, Abhishek Das, Georgia Gkioxari, Stefan Lee, Irfan Essa, Devi Parikh, and Dhruv Batra. Embodied question answering in photorealistic environments with point cloud perception. In Proceedings of the IEEE/CVF Conference on Computer Vision and Pattern Recognition, pages 6659–6668, 2019. 18
- [77] Erik Wijmans, Abhishek Kadian, Ari Morcos, Stefan Lee, Irfan Essa, Devi Parikh, Manolis Savva, and Dhruv Batra. DD-PPO: Learning near-perfect pointgoal navigators from 2.5 billion frames. In *International Conference on Learning Representations (ICLR)*, 2020. 6, 7
- [78] Qiaoyun Wu, Xiaoxi Gong, Kai Xu, Dinesh Manocha, Jingxuan Dong, and Jun Wang. Towards target-driven visual navigation in indoor scenes via generative imitation learning. *IEEE Robotics and Automation Letters*, 6(1):175– 182, 2020. 2
- [79] Yuchen Wu, Pengcheng Zhang, Meiying Gu, Jin Zheng, and Xiao Bai. Embodied navigation with multi-modal in-

- formation: A survey from tasks to methodology. *Information Fusion*, page 102532, 2024. 1, 2, 18
- [80] Dejing Xu, Zhou Zhao, Jun Xiao, Fei Wu, Hanwang Zhang, Xiangnan He, and Yueting Zhuang. Video question answering via gradually refined attention over appearance and motion. In ACM Multimedia, 2017. 18
- [81] Jun Xu, Tao Mei, Ting Yao, and Yong Rui. Msr-vtt: A large video description dataset for bridging video and language. In Proceedings of the IEEE conference on computer vision and pattern recognition, pages 5288–5296, 2016. 6
- [82] Zifan Xu, Bo Liu, Xuesu Xiao, Anirudh Nair, and Peter Stone. Benchmarking reinforcement learning techniques for autonomous navigation. In 2023 IEEE International Conference on Robotics and Automation (ICRA), pages 9224–9230. IEEE, 2023. 2
- [83] Karmesh Yadav, Arjun Majumdar, Ram Ramrakhya, Naoki Yokoyama, Alexei Baevski, Zsolt Kira, Oleksandr Maksymets, and Dhruv Batra. Ovrl-v2: A simple stateof-art baseline for imagenav and objectnav. arXiv preprint arXiv:2303.07798, 2023. 6, 7
- [84] Karmesh Yadav, Ram Ramrakhya, Arjun Majumdar, Vincent-Pierre Berges, Sachit Kuhar, Dhruv Batra, Alexei Baevski, and Oleksandr Maksymets. Offline visual representation learning for embodied navigation. In Workshop on Reincarnating Reinforcement Learning at ICLR 2023, 2023. 6, 7
- [85] Naoki Yokoyama, Sehoon Ha, Dhruv Batra, Jiuguang Wang, and Bernadette Bucher. Vlfm: Vision-language frontier maps for zero-shot semantic navigation. In 2024 IEEE International Conference on Robotics and Automation (ICRA), pages 42–48. IEEE, 2024. 19
- [86] Naoki Yokoyama, Ram Ramrakhya, Abhishek Das, Dhruv Batra, and Sehoon Ha. Hm3d-ovon: A dataset and benchmark for open-vocabulary object goal navigation. arXiv preprint arXiv:2409.14296, 2024. 18, 19
- [87] Bangguo Yu, Hamidreza Kasaei, and Ming Cao. L3mvn: Leveraging large language models for visual target navigation. In 2023 IEEE/RSJ International Conference on Intelligent Robots and Systems (IROS), pages 3554–3560. IEEE, 2023. 16
- [88] Zhou Yu, Dejing Xu, Jun Yu, Ting Yu, Zhou Zhao, Yueting Zhuang, and Dacheng Tao. Activitynet-qa: A dataset for understanding complex web videos via question answering. In *Proceedings of the AAAI Conference on Artificial Intelligence*, pages 9127–9134, 2019. 18
- [89] Zhou Yu, Jun Yu, Yuhao Cui, Dacheng Tao, and Qi Tian. Deep modular co-attention networks for visual question answering. In *Proceedings of the IEEE/CVF conference on computer vision and pattern recognition*, pages 6281–6290, 2019. 7
- [90] Kuo-Hao Zeng, Zichen Zhang, Kiana Ehsani, Rose Hendrix, Jordi Salvador, Alvaro Herrasti, Ross Girshick, Aniruddha Kembhavi, and Luca Weihs. Poliformer: Scaling on-policy rl with transformers results in masterful navigators. arXiv preprint arXiv:2406.20083, 2024. 2, 3, 5, 7, 20
- [91] Hang Zhang, Xin Li, and Lidong Bing. Video-llama: An

- instruction-tuned audio-visual language model for video understanding. arXiv preprint arXiv:2306.02858, 2023. 7
- [92] Jiazhao Zhang, Chenyang Zhu, Lintao Zheng, and Kai Xu. Rosefusion: random optimization for online dense reconstruction under fast camera motion. ACM Transactions on Graphics (TOG), 40(4):1–17, 2021. 17
- [93] Jiazhao Zhang, Yijie Tang, He Wang, and Kai Xu. Asrodio: Active subspace random optimization based depth inertial odometry. *IEEE Transactions on Robotics*, 39(2): 1496–1508, 2022. 17
- [94] Jiazhao Zhang, Liu Dai, Fanpeng Meng, Qingnan Fan, Xuelin Chen, Kai Xu, and He Wang. 3d-aware object goal navigation via simultaneous exploration and identification. In Proceedings of the IEEE/CVF Conference on Computer Vision and Pattern Recognition, pages 6672–6682, 2023. 1
- [95] Jiazhao Zhang, Kunyu Wang, Rongtao Xu, Gengze Zhou, Yicong Hong, Xiaomeng Fang, Qi Wu, Zhizheng Zhang, and He Wang. Navid: Video-based vlm plans the next step for vision-and-language navigation. *Robotics: Science and Systems*, 2024. 3, 4, 5, 6, 15, 16, 18, 19, 20
- [96] Yue Zhang, Ziqiao Ma, Jialu Li, Yanyuan Qiao, Zun Wang, Joyce Chai, Qi Wu, Mohit Bansal, and Parisa Kordjamshidi. Vision-and-language navigation today and tomorrow: A survey in the era of foundation models. *ArXiv*, abs/2407.07035, 2024. 1, 2
- [97] Zhen Zhang, Jiaqing Yan, Xin Kong, Guangyao Zhai, and Yong Liu. Efficient motion planning based on kinodynamic model for quadruped robots following persons in confined spaces. *IEEE/ASME Transactions on Mechatronics*, 26(4): 1997–2006, 2021. 2
- [98] Duo Zheng, Shijia Huang, Lin Zhao, Yiwu Zhong, and Liwei Wang. Towards learning a generalist model for embodied navigation. arXiv preprint arXiv:2312.02010, 2023. 1, 2, 3, 7
- [99] Lintao Zheng, Chenyang Zhu, Jiazhao Zhang, Hang Zhao, Hui Huang, Matthias Niessner, and Kai Xu. Active scene understanding via online semantic reconstruction. In *Computer Graphics Forum*, pages 103–114. Wiley Online Library, 2019. 17
- [100] Gengze Zhou, Yicong Hong, and Qi Wu. Navgpt: Explicit reasoning in vision-and-language navigation with large language models. *arXiv preprint arXiv:2305.16986*, 2023. 1, 2, 3, 14
- [101] Gengze Zhou, Yicong Hong, Zun Wang, Xin Eric Wang, and Qi Wu. Navgpt-2: Unleashing navigational reasoning capability for large vision-language models. In *European Conference on Computer Vision*, pages 260–278. Springer, 2025. 3, 14
- [102] Deyao Zhu, Jun Chen, Kilichbek Haydarov, Xiaoqian Shen, Wenxuan Zhang, and Mohamed Elhoseiny. Chatgpt asks, blip-2 answers: Automatic questioning towards enriched visual descriptions, 2023. 3
- [103] Weiqin Zu, Wenbin Song, Ruiqing Chen, Ze Guo, Fanglei Sun, Zheng Tian, Wei Pan, and Jun Wang. Language and sketching: An Ilm-driven interactive multimodal multitask robot navigation framework. In 2024 IEEE International Conference on Robotics and Automation (ICRA), pages 1019–1025. IEEE, 2024. 15

Contents

1. Introduction	1
2. Related Works	2
3. Method	3
3.1. Model of Uni-NaVid	4
3.2. Training of Uni-NaVid	5
3.3. Implementation Details	5
4. Experiment	6
4.1. Individual Task Results	6
4.2. Qualitative Results in Real-World	7
4.3. Ablation Study	8
5. Conclusion	8
6. Task Definition	14
6.1. Vision-and-language Navigation (VLN)	14
6.2. Object Goal Navigation (ObjectNav)	14
6.3. Embodied Question Answering (EQA)	14
6.4. Human Following	15
7. Implementation Details	15
7.1. Online Visual Token Merging	15
7.2. Token Organization	15
7.3. Traing Strategy	15
8. Data Preparation Details	16
8.1. Data Collection	16
8.2. Instruction Augmentation	17
9. Real-world deployment	17
9.1. Robot Setup	17
9.2. Real-world System Architecture	17
10Experiments	18
10.1Experiment Setup	18
10.1.1 Benchmark.	18
10.1.2 Metrics.	18
10.2Real-world Experiments	18
10.3More Benchmark Experiments	19
10.4More Ablation study	20
10.5Time Analyze	20
10.6Qualitative Experiments	20

6. Task Definition

We introduce the details of four embodied navigation tasks that are included in our paper.

6.1. Vision-and-language Navigation (VLN)

Vision-and-language navigation [37] requires the agent to follow the instruction by moving between given landmarks and stopping at the described destination within unseen environments. The instruction of VLN is at free-form which describes a trajectory of landmarks and the motions between these landmarks. The landmarks and motions are open-vocabulary. VLN is widely regarded as a challenging task because it has to understand the free-form instruction, align the navigation history with instruction, and do path planning. Despite the fact that many works consider using pre-build landmark graphs [51, 100, 101] to simplify VLN, we consider a more practical setting that uses a continuous environment (VLN-CE [37]). Currently, there are two mainstream VLN-CE datasets: VLN-CE R2R [37] and VLN-CE RxR [40]. We provide examples of these instructions:

- VLN-CE R2R: Walk down the hallway along the banister railing on the upper floor of the home. Walk through the open door next to the staircase. Walk into the room, which has a couch and chairs around a coffee table.
- VLN-CE RxR: You are starting in the corner of a living room. Turn around to find a clock hanging on the wall in the hallway. Take two steps toward it. Turn right and walk straight, passing between the blue couch and the kitchen. You should now be looking through windows into the backyard. To your right is an open patio, and to your left are four framed black-and-white pictures. You've completed the instructions.

In the benchmark VLN-CE R2R and VLN-CE RxR, the agent is required to navigate each of the landmarks in the given order of the instruction and stop within 3 meters of the destination. The max navigation step is 500 steps.

6.2. Object Goal Navigation (ObjectNav)

In ObjectNav [64], an agent is initialized at a random starting position and orientation in an unseen environment and asked to find an instance of an object category ('find a chair') by navigating to it. The agent should explore the environments to track the location location that could locate target objects, and then identify the target object and stop nearby. Specifically, we follow the Habitat-matterport 3D dataset, which requires the agent to search a specific category object, which could be one of a category set including couch, bed, chair, toilet, plant, and TV. In the benchmark HM3D, the trajectory is considered a success if the target stops within 1 meter of the target object under 500 steps.

6.3. Embodied Question Answering (EQA)

Embodied Question Answering [18] is a complicated task, which involves answering questions by interacting with and navigating within an unseen 3D environment. Following the setting of MP3D-EQA, the agent is first given a question

related to an object, like the color or location, and then the agent is required to identify the described target and return a natural language that directly answers the question. Here are some examples of the questions:

- What room is the chair located in?
- What color is the bed?
- What color is the couch in the living room?

In the benchmark MP3D-EQA, the agent is required to find the target and answer the question within 500 steps. And the episode will be considered a success if the answer matches the GT answer.

6.4. Human Following

The three tasks discussed above primarily address static and fixed scenarios, with limited applicability to dynamic environments. In contrast, human following [23, 31, 103], as a classic robot target tracking problem, focuses on enabling robots to interact effectively in dynamic settings, making it particularly well-suited for real-world applications.

Traditional human following tasks often rely on modular-based approaches [27], mainly focusing on the robot's following strategies [71] and controller design [34]. These studies typically assume that the target to be tracked is either known or specified at the beginning, an assumption that fails to account for the complexities of real-world environments. In this paper, we introduce a novel human-following task driven by natural language instruction, where the robot should locate and follow a specific human that aligns with the given description in a potentially crowded and dynamic environment.

We developed a benchmark for this task based on Habitat 3.0 [56]. In each episode, multiple humans with diverse characteristics are randomly placed in the scene, and the robot is initialized near the target human to be followed, ensuring that this human is within the robot's initial observation. The robot interprets natural language instructions, such as "follow the man wearing a blue shirt and black pants" or "stay behind the woman in yellow", to locate the individual that best matches the description. It then tracks and follows the person's movements, dynamically adapting until reaching the pre-defined navigation goal. An episode is deemed successful if the robot stops within 2 meters of the correct human and faces him/her at the end.

7. Implementation Details

In this section, we provide more implementation details of Uni-NaVid.

7.1. Online Visual Token Merging

Online visual token merging is the key technique of Uni-NaVid to enable efficient encoding of a long horizon of ego-centric videos. We provide an algorithm in Algo. 1. Specifically, we organize the online captured frames. When

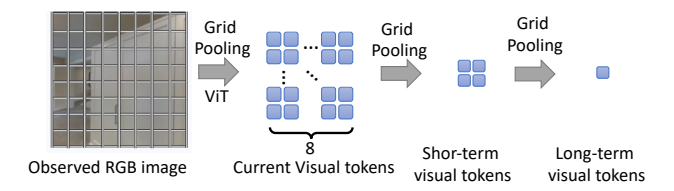


Figure 6. **Grid pooling**. We add a visualization of grid pooling across different types of observations.

the model only receives one frame, that frame becomes the current observation. Then we extract the visual tokens and leverage grid pooling (See Fig. 6). We split the image into 8×8 and ach grid is conducted an average operation, leading to the final 64 tokens for current observations. Then with more incoming frames, we perform grid pooling to older current observation tokens, which leads to 2×2 tokens, and append them into a short-term memory buffer.

If the time step is over 65 steps, then the oldest short-term frame will be pooped out and then is performed grid pooling to 1 token. This token is a long-term visual token which then will be inserted into the long-term visual token list if the long-term visual token list is empty or the cos similarity is smaller than τ . Here, we use $\tau=0.95$, which is obtained empirically [69], which achieves a balance between the efficiency and effective.

7.2. Token Organization

To facilitate the understanding of the large language model, we have to organize the tokens, including observation tokens, instruction tokens, and special tokens. Specifically, we use observation indicator tokens to indicate the following parts are visual tokens. Besides, we add an image separator token between the adjacent visual tokens of each frame (following existing VLMs [24, 48]), this is crucial to distinguish the visual information inherent from different frames. Finally, if the task is navigation, we add a navigation special token <NAV> to indicate the task is navigation. Once the model understands the navigation special token, it will directly output action tokens.

Note that, it is important to use a navigation special token which could address the ambiguity problem under the embodied question-answering task because a large language model could confused about whether to directly answer the question or output actions to the target. The supported experiments can be found in the main paper Table 9.

7.3. Traing Strategy

We follow the training strategy of NaVid [95] in a two-stage manner. In the first stage, we firstly pre-train the projector of Uni-NaVid with the Image QA dataset then finetune both the projector and LLM with the Video QA dataset. We

Algorithm 1 Online Visual Token Merging

Require:

- \bullet Total number of frames T
- Short memory buffer length B
- Grid pooling scales: α_{curr} , α_{short} , α_{long}
- Current visual tokens: $\mathbf{X}_T \in \mathbb{R}^{N_x \times C}$
- Previously merged tokens: X_{curr} , X_{short} , X_{long}
- Number of frames merged in the last tokens of long memory: K

Ensure:

- Updated merged tokens: X'_{curr} , X'_{short} , X'_{long}
- Updated number of frames merged in the last tokens of long memory: K'

```
1: if T == 1 then
                       \mathbf{X}'_{\text{short}}, \mathbf{X}'_{\text{long}} \leftarrow []
  3:
                      \mathbf{X}_{curr \rightarrow short} \leftarrow GridPool(\mathbf{X}_{curr}, \frac{\alpha_{short}}{\alpha_{curr}})
   4:
                      \mathbf{X}'_{\text{short}} \leftarrow \mathbf{X}_{\text{short}} + [\mathbf{X}_{\text{curr} \rightarrow \text{short}}]
   5:
   6: end if
          \mathbf{X}'_{\text{curr}} \leftarrow GridPool(\mathbf{X}_T, \alpha_{\text{curr}})
   8: if T > B + 1 then
                      \mathbf{X}_{\text{short} \rightarrow \text{long}} \leftarrow GridPool(\mathbf{X}_{\text{short}}[0], \frac{\alpha_{\text{long}}}{\alpha_{\text{short}}})
                      \mathbf{X}_{short}' \leftarrow \mathbf{X}_{short}[1:]
 10:
                      s \leftarrow \cos(\mathbf{X}_{\text{long}}[-1], \mathbf{X}_{\text{short} \rightarrow \text{long}})
 11:
                      if T > B + 2 and s > \tau then
 12:
                                \begin{aligned} \mathbf{X}_{\text{last\_long}} &\leftarrow \frac{1}{K+1} (K \mathbf{X}_{\text{long}} [-1] + \mathbf{X}_{\text{short} \rightarrow \text{long}}) \\ \mathbf{X}'_{\text{long}} &\leftarrow \mathbf{X}_{\text{long}} [:-1] + [\mathbf{X}_{\text{last\_long}}] \\ K' &\leftarrow K+1 \end{aligned}
 13:
 14:
 15:
 16:
                                 \begin{aligned} \mathbf{X}_{long}' \leftarrow \mathbf{X}_{long} + [\mathbf{X}_{short \rightarrow long}] \\ K' \leftarrow 1 \end{aligned}
 17:
 18:
                       end if
 19:
20: end if
```

collect the data from LLama-Vid [44] and Pandm [16]. In the second state, we train both projector and LLM with collected navigation data. The default parameters are borrowed from NaVid [95].

8. Data Preparation Details

To train Uni-NaVid, we required massive navigation data across different navigation tasks. It is extremely challenging to collect a large number of high-quality annotated data in the real world. Therefore, we collect navigation data in the synthetic environments and we describe the details in the following sections.

8.1. Data Collection

Navigation samples. We define the navigation samples including a navigation history video, corresponding instruc-

tions, and future actions (we use four actions). Here the navigation history video is accumulated frames to time step T, which can be indicated as a set of frames $\{\mathbf{x}_t\}_{1:T}$

Vision-and-language navigation. We collect VLN navigation samples in the VLN-CE simulator [37, 63]. We use the training split of R2R dataset [37] and RxR dataset [39], which include the ground-truth navigation trajectory and corresponding instructions within the HM3D datasets [57]. Therefore, we deploy the agent to follow the GT trajectory and render RGB images during navigation. In this case, we collect 0.64 M navigation video-action samples.

Besides GT navigation samples, we also use DAG-GER [62] to collect more diverse navigation samples, nearly 1.69 M navigation samples. Specifically, we run Uni-NaVidin the training split and collect the expert actions by using a deterministic path planning method [65] to the next non-arrived landmark.

We also collect a sub-split (70k) of previously collected VLN data (randomly sample the trajectories which are smaller than 20 steps) and augment the instruction with low-level actions, e.g., "move forward 4 steps, then turn right 3 steps.". We find that Uni-NaVidcan easily master the low-level instructions, but the performance drops when the low-level instruction expands significantly.

Object goal navigation. We collect the object goal navigation data in the HM3D datasets [57] in Habitat simulator [63]. Here, the agent is initialized in unseen environments and is required to find one object that could be a category set of chair, couch, TV, toilet, bed, and plant. We deploy L3MVN [87] in the HM3D training split and collect the navigation trajectory. We only collect 483 k navigation trajectory which is successful in finding the target. And we use the instruction template: "Search for a/an [Object]." Note that, using the shortest path to the target object as the navigation video samples leads to an extremely low performance (30.1% SR) because the model can not learn to explore or recover from mistakes.

Embodied question answering. We collect 240 k video-action samples from MP3D-EQA dataset [18] and 10 k video-answering samples. The video-action samples are rendered based on the GT trajectory of MP3D-EQA, and use the question as the instruction. And the video-answering samples are rendered frames of full trajectory, and we use the GT answering as the answer of large language model of MP3D-EQA.

Human following. We collect 544 k video-action samples from a self-build human following environment based on the Habitat 3.0 simulator. Specifically, we generate a large amount of human-following data based on the HM3D dataset [57]. For each episode, we first determine the total number of humans (2–6) based on the area of the scene, assign an ID to the target human to be followed, and specify the language instruction. Next, we randomly initialize the

starting positions of the humans in the scene and place the robot near the target human, ensuring that the target is visible in the robot's camera view. Finally, we randomly generate multiple navigation waypoints for each human and use a low-level path planner to guide them to these waypoints sequentially. During this process, the robot continuously receives the target human's position in each step and uses a local planner to follow the human while avoiding obstacles nearby until the human reaches the final waypoint.

8.2. Instruction Augmentation

We collect instructions from various datasets, and the quality of the instructions is limited in diversity. Especially for object goal navigation, the fixed template could cause the instruction to become a task indicator, which could damage the performance. In this case, we use ChatGPT, to augment the instructions. The prompts are listed as follows:

Given a robot navigation task instruction, rephrase the instruction to make its grammar and structure more diverse while preserving its original meaning. Additionally, ensure all grammatical errors in the instruction are corrected. Use varied sentence structures and descriptions for objects and directions to enhance linguistic diversity. Keep the instructions clear and concise to ensure they remain suitable for a robot navigation system.

We find the instruction augmentation could increase the performance of VLN (+2.31% in SR) and ObjectNav(+3.7% in SR). We believe the cross-dataset instruction augmentation could be a promising topic to further investigate.

9. Real-world deployment

9.1. Robot Setup.

We provide a visualization of our robotic dog in Fig. 7. Our robotic dog is Unitree GO2 and we mount a RealSense D455 camera on the head of the robotic dog. Here, we only use the RGB frames with a resolution of 640×480 in the setting of 90° HFOV. We also mount a portable Wi-Fi at the back of the robot dog, which is used to communicate with the remote server (send captured images and receive commands). Unitree GO2 is integrated with a LiDAR-L1, which is only used for local motion planning.

Note that Uni-NaVid does not rely on any odometry algorithms [92, 93] or noiseless depth [41, 64, 99], making it easy to deploy in real-world environments.

9.2. Real-world System Architecture

We provide a visualization of the real-world setup in Fig. 8. Our model is deployed on a remote server equipped with an

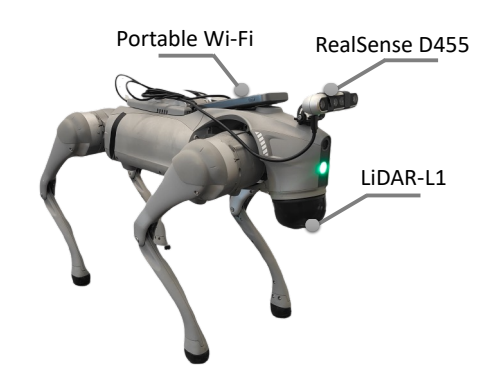


Figure 7. **Robot setup.** We use Unitree GO2 as our embodiment, and we mount RealSense D455, a portable Wi-Fi and a LiDAR-L1. Note that, our model only takes RGB frames as input. The portable Wi-Fi is used for communication with the remote server and the Lidar is used for the local controller API of Unitree Dog.

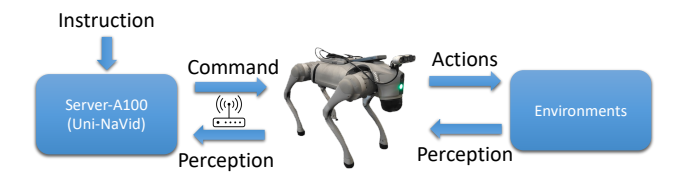


Figure 8. **Real-world system architecture.** We deploy our model at a remote server, and the robot communicates with the server through the Internet.

NVIDIA A100 GPU. During navigation, the server receives navigation instructions and images captured by the robotic dog through the Internet. To ensure efficient communication, the images are compressed before transmission. After processing the newly captured images, the model generates action commands (FORWARD, LEFT, RIGHT, and STOP) and sends them to the robotic dog. Upon receiving these commands, the robotic dog executes the actions using a local motion planning model (specifically, the off-the-shelf model provided by Unitree Dog). Leveraging our online token merging strategy, the model processes newly captured images efficiently, requiring approximately 0.2 seconds for inference, while Internet communication (image transmission and command reception) takes about 0.3 seconds.

Non-blocking navigation. After receiving a set of four action commands, the robotic dog executes them sequentially. Upon completing each action, the robot captures a new image and transmits it to the server. In cases where multiple action commands are generated for a single step, the robot prioritizes and executes the most recent command, as it reflects the latest planning outcome.

10. Experiments

10.1. Experiment Setup

10.1.1. Benchmark.

We conduct extensive experiments on public benchmarks across different tasks. We celebrate them as follows:

- Vision-and-language navigation. We conduct experiments on the Val-Unseen split of VLN-CE R2R (Main paper Table 2) and RxR (Main paper Table 3). They contain novel environments and novel instructions.
- Object goal navigation. In the main paper (Table 4), we conduct experiments on the validation set of the HM3D object goal navigation dataset. In the Supplementary, we also conduct experiments (Table 12) on HM3D-OVON [86], which is an open-vocabulary object goal navigation benchmark.
- Embodied Question answering. We conduct experiments on the validation set of the MP3D-EQA [76], where the questions and scenes are novel. Besides, we also conduct experiments (Table 13) on OpenEQA [53], which is a benchmark to evaluate the performance of understanding the marionettes with egocentric video.
- Human following. In Table 5 of the main paper, the experiment is conducted on a self-build benchmark based on the HM3D dataset, which also served as the source of the training dataset. Additionally, we also build two benchmarks based on the HSSD dataset and MP3D dataset, respectively, and evaluate the human following capability of Uni-NaVid across different datasets and scenes (Table 14).

10.1.2. Metrics.

We use the default metrics of each benchmark. For vision-and-language navigation and object goal navigation, [37, 64, 79], we use SR, OSR, and SPL as metrics. Specifically, SR (Success Rate) measures the proportion of tasks in which the agent successfully reaches the target location (in VLN the distance threshold is 3 m, and in ObjectNav is 1 m) within the allowed time steps (Up to 500 steps). OSR (Oracle Success Rate) extends SR by accounting for the agent's proximity to the goal, considering the task successful if the agent is close enough, even without directly stopping at the target. SPL (Success weighted by Path Length) evaluates the agent's efficiency by combining success with the optimality of its trajectory, penalizing longer-than-necessary paths while rewarding those closer to the shortest possible route.

For human following navigation, we use SR, FR, and CR metrics. SR (Success Rate) measures the proportion of events in which the agent successfully follows the target human to the endpoint. FR (Following Rate) refers to the proportion of steps in which the agent successfully follows the target human for each step. CR (Collision Rate) refers to

the proportion of episodes in which the agent collides with the human during the movement.

For embodied question answering, we use ACC metric, which directly measures the percentage of correct answers. For ScnaQA [7], we use EM, BLUE, ROUGE, METEOR, CIDEr as metrics. Specifically, EM (Exact Match) evaluates the percentage of predictions that exactly match the reference answers. BLEU (Bilingual Evaluation Understudy) measures the n-gram overlap between the generated text and the reference, rewarding precise matches in shorter sequences. ROUGE (Recall-Oriented Understudy for Gisting Evaluation) assesses the overlap of word sequences, focusing on recall and capturing the informativeness of the generated text. METEOR (Metric for Evaluation of Translation with Explicit ORdering) combines precision and recall, using synonym matching and stemming to account for variations in phrasing. Lastly, CIDEr (Consensus-based Image Description Evaluation) measures the similarity of generated responses to multiple references by capturing human consensus, emphasizing relevance and diversity in the output.

For video-question answering benchmark MSVD-QA [80], MSRVTT-QA [80], and ActivityNet-QA [88], we use ACC and Score metrics. Specifically, ACC (Accuracy) measures the proportion of correctly answered questions, providing a straightforward assessment of the model's overall correctness. Score, on the other hand, evaluates the quality of the generated answers using GPT (GPT 3.5 in implementation) as the zero-shot evaluation assistor to assign relative scores on a scale of 1 to 5 for generated answers.

10.2. Real-world Experiments

We conduct real-world experiments to study the generalizability of our method in the real world. Specifically, we leverage the VLN task, which includes both landmarks and motions, to evaluate our method with the previous VLN method NaVid [95]. Following previous work [95], we designed two types of instructions for different difficulties (25 simple instructions and 25 complex instructions). The simple instructions, which require the agent to navigate to a single robot landmark and stop; (2) complex instructions, which require the agent to follow a series of simple instructions.

We list some examples of used instructions in experiments. Simple instruction examples:

- Move forward 1 step, then stop.
- Turn left 5 steps, then stop.
- Move to the right chair, then turn left. Complex instructions:
- Move forward 5 steps, then turn left 4 steps, and finally turn right 5 steps.
- Go straight to the chair, then turn right and move to the door, stop by the door.

Method	Simple Ins.	Complex Ins.
NaVid [95]		20%
Uni-NaVid	92%	84%

Table 10. **Real-world VLN experiments.** We compare our method with NaVid on two types of instructions: simple instructions (25) and complex instructions (25).

Method	Observation			VLN-CE RxR Val-Unseen				
	Odom.	Depth	S.RGB	TL	$NE\downarrow$	$\mathbf{OS} \!\!\uparrow$	$\textbf{SR} \!\!\uparrow$	$\textbf{SPL} \!\!\uparrow$
LAW [60]	√	√	✓	4.01	10.87	21.0	8.0	8.0
CM2 [21]	✓	\checkmark	\checkmark	12.29	8.98	25.3	14.4	9.2
WS-MGMap [14]	✓	\checkmark	\checkmark	10.80	9.83	29.8	15.0	12.1
ETPNav.FF [75]	✓	\checkmark	\checkmark	-	8.79	36.7	25.5	18.1
Seq2Seq [37]		\checkmark	\checkmark	1.16	11.8	5.02	3.51	3.43
CMA [37]		\checkmark	\checkmark	5.09	11.7	10.7	4.41	2.47
A^2 Nav [†] [15]			\checkmark	-	-	-	16.8	6.3
NaVid [95]			\checkmark	10.59	8.41	34.5	23.8	21.2
Uni-NaVid			\checkmark	8.3	8.08	40.9	29.5	28.1

Table 11. **Vision-and-language navigation (RxR).** Comparison on VLN-CE RxR [40] Val-Unseen. †: indicates zero-shot methods

• Turn a large right, and go forward to a plant, then right at the plant and move to the TV, stop close to TV.

Here we present our results in Table 10. We find that both Navid and our method can achieve high SR in simple instructions, However, for complex instructions, our method shows significant improvements. This demonstrates the superiority of our method over existing methods. We add more visual results to the attached video.

10.3. More Benchmark Experiments

Cross-dataset Vision-and-Language Navigation Evaluation. We evaluate the cross-dataset performance of our method on VLN-CE RxR by excluding the VLN-CE RxR data at training time. The results are presented in Table 11. Notably, even without training on RxR, our method still outperforms existing approaches. However, a significant decrease in all metrics is observed compared to when RxR training data is included. We hypothesize that this discrepancy arises from differences in trajectory characteristics: trajectories in the R2R dataset have relatively uniform lengths (approximately 10 meters), whereas those in RxR exhibit greater diversity, ranging from approximately 2 meters to 20 meters. This disparity constrains our method's performance on the RxR dataset and underscores the importance of training on diverse trajectories.

Open-vocabulary Object goal navigation. To test the general ability of searching, we evaluate our method on the open-vocabulary object goal navigation benchmark HM3D-OVON [86]. Here, our method is evaluated in a zero-shot manner, and the results are presented in Tab. 12. We find that our method archives SOTA-level performance even without training with the training data. Compared with VLFM [85] which is also a zero-shot deployed, our method

Method	VAL SEEN		VAL SEEN SYNONYMS		VAL UNSEEN	
	SR↑	SPL↑	SR↑	SPL↑	SR↑	SPL↑
BC	11.1	4.5	9.9	3.8	5.4	1.9
DAgger	11.1	4.5	9.9	3.8	5.4	1.9
RL	18.1	9.4	15.0	7.4	10.2	4.7
BCRL	39.2	18.7	27.8	11.7	18.6	7.5
DAgRL	41.3	21.2	29.4	14.4	18.3	7.9
VLFM* [85]	35.2	18.6	32.4	17.3	35.2	19.6
DAgRL+OD [86]	38.5	21.1	39.0	21.4	37.1	19.8
Uni-NaVid*	41.3	21.1	43.9	21.8	39.5	19.8

Table 12. **Object goal navigation.** Comparison on HM3D-OVON [86]. * : denotes zero-shot methods.

	EM-EQA					
Method	ScanNet	HM3D	ALL			
	Eq. (1)	Eq. (1)	Eq. (1)			
Blind LLMs						
GPT-4	32.5	35.5	33.5			
LLaMA-2	27.9	29.0	28.3			
Socratic LLMs w/ Frame Captions						
GPT-4 w/ LLaVA-1.5	45.4	40.0	43.6			
LLaMA-2 w/ LLaVA-1.5	39.6	31.1	36.8			
Socratic LLMs w/ Scene-Graph Captions						
GPT-4 w/ CG	37.8	34.0	36.5			
LLaMA-2 w/ CG	31.0	24.2	28.7			
GPT-4 w/ SVM	40.9	35.0	38.9			
LLaMA-2 w/ SVM	36.0	30.9	34.3			
Multi-Frame VLMs						
GPT-4V	51.3	46.6	49.6			
Human Agent	87.7	85.1	86.8			
Uni-NaVid	41.4	38.1	40.3			

Table 13. **Embodied video question answering.** Comparison on OpenEQA benchmark. EM-EQA results are broken down by data source (ScanNet, HM3D, and ALL). GPT-4V scores are calculated on a subset of 500 OpenEQA questions due to API limitations.

archives significant improvements on all splits. This proves the generalizability of our methods.

OpenEQA benchmark [53]. To further evaluate our method on embodied question answering, we conduct experiments in OpenEQA, which require the methods to answer questions by analyzing an egocentric video. The results are shown in Tab. 13. We find our method achieves competitive performance to the strongest commercial used Vision-Language model such as GPT-4V. Besides, by directly observing and understanding the video sequences, our method does not need additional frame caption or Socratic-style promoted [53] used in other LLMs.

Cross-Environments Following. We evaluate our method in novel environments, including HSSD [35] (synthetic environments) and MP3D [10] (reconstructed environments). The results, presented in Table 14, demonstrate that our approach consistently outperforms baseline methods in both SR and FR metrics across HSSD and MP3D. Notably, our method achieves significant improvements in HSSD, likely due to the absence of reconstruction artifacts in synthetic

Method	HF-HSSD			HF-MP3D		
Menion	SR↑	FR↑	CR↓	SR↑	FR↑	CR↓
PoliFormer [90]	2.67	20.81	0.97	2.62	16.59	1.43
PoliFormer* [90]	26.97	54.20	10.01	25.42	47.80	8.72
PoliFormer† [90]	27.10	53.96	9.34	21.90	41.42	7.15
IBVS* [23]	66.32	80.26	0.19	56.86	68.91	1.33
IBVS† [23]	65.36	80.33	0.15	58.15	65.83	0.77
Uni-NaVid	81.65	89.34	1.33	69.80	78.96	2.99

Table 14. **Human following.** Comparison on Human Following HSSD Benchmark (HF-HSSD) and Human Following MP3D Benchmark (HF-MP3D). *: Methods use GroundingDINO [49] as the open-vocabulary human detector. †: Methods use the groundtruth bounding box provided by the simulator.

Design	VLN (SR↑)	ObjNav (SR↑)	EQA (ACC↑)	Follow (SR↑)
4 tokens for Curr. Obs.	43.4	50.2	40.5	-
1 token for Curr. Obs.	35.1	45.3	31.2	-
1 token for Short. Obs.	46.2	69.2	44.9	60.3
$\tau = 0.9$	40.2	70.0	43.2	57.8
τ =0.95	48.7	73.7	47.3	61.2
τ =0.99	49.6	70.2	48.1	57.2

Table 15. **Ablation study** of token number and τ

environments, which reduces the likelihood of the robot being stuck. For the CR (collision rate) metric, IBVS adopts a highly conservative strategy that maintains a considerable distance from the target (i.e., a large bounding box). While this results in a lower CR, it adversely affects FR and SR performance.

10.4. More Ablation study

We conduct additional ablation studies to validate the effectiveness of our key design components. The results are presented in Table 15. Notably, we observed a significant performance drop when the number of current observation tokens was reduced. In particular, the following task failed across all sequences, potentially due to the inability of a smaller number of tokens to provide sufficient information for tracking human motion. Furthermore, we found that increasing the value of τ led to improved performance. This outcome is intuitive, as a higher τ retains more long-term observation tokens, which are crucial for understanding navigation history.

10.5. Time Analyze

To evaluate the efficiency of our method, we present the average running time and token count across different time steps in Fig. 9. Our approach is compared against existing models that also employ token merging strategies. The results demonstrate that our method is more efficient which achieves an inference time of approximately 0.2 seconds. Moreover, our method maintains consistent running times, whereas the running times of existing methods increase significantly. These advantages stem from two key factors: *First*, our model architecture is highly effi-

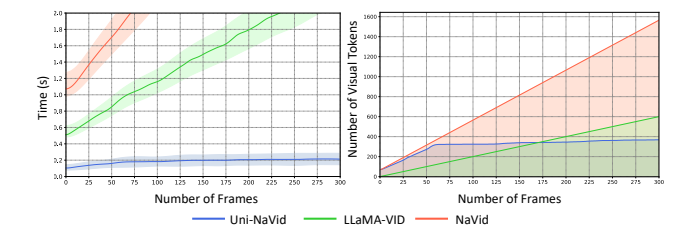


Figure 9. **Time efficiency visualization.** We provide the average running time and the number of tokens across different time steps.

cient, whereas other approaches, such as LLaMA-VID [44] and NaVid [95], rely on time-consuming operations like QFormer. *Second*, our online token merging strategy results in a gradual increase in token count, ensuring more stable inference times.

10.6. Qualitative Experiments

We provide visual results of our method on various benchmarks: Fig.10 illustrates results for VLN-CE R2R and RxR, Fig.11 for HM3D ObjectNav, and Fig. 12 for MP3D-EQA, Fig. 13 for HM3D human following. For additional visual results, please refer to the attached video.

Vision-and-language Navigation

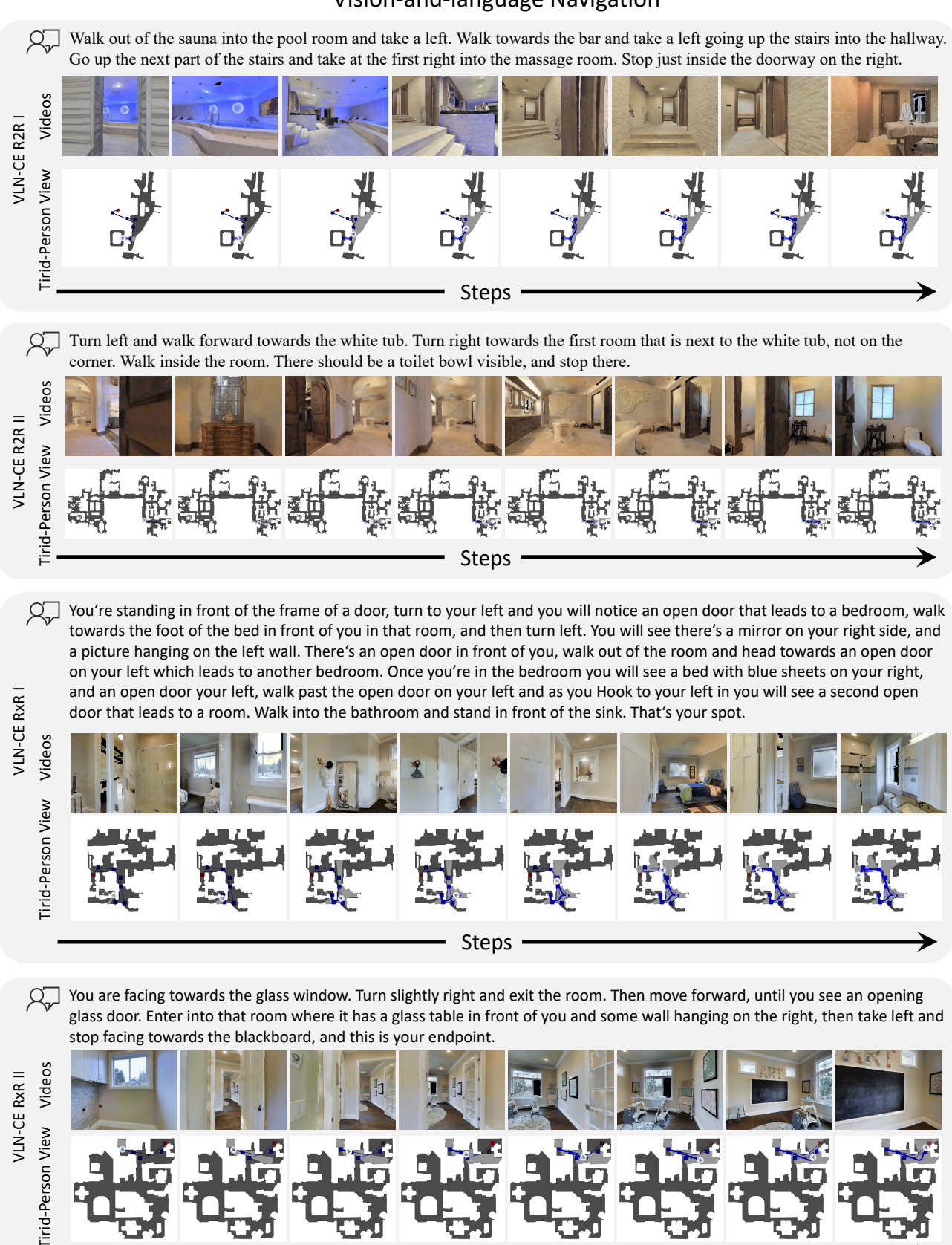


Figure 10. Visual results of VLN on VLN-CE R2R and RxR.

Steps

Object goal navigation

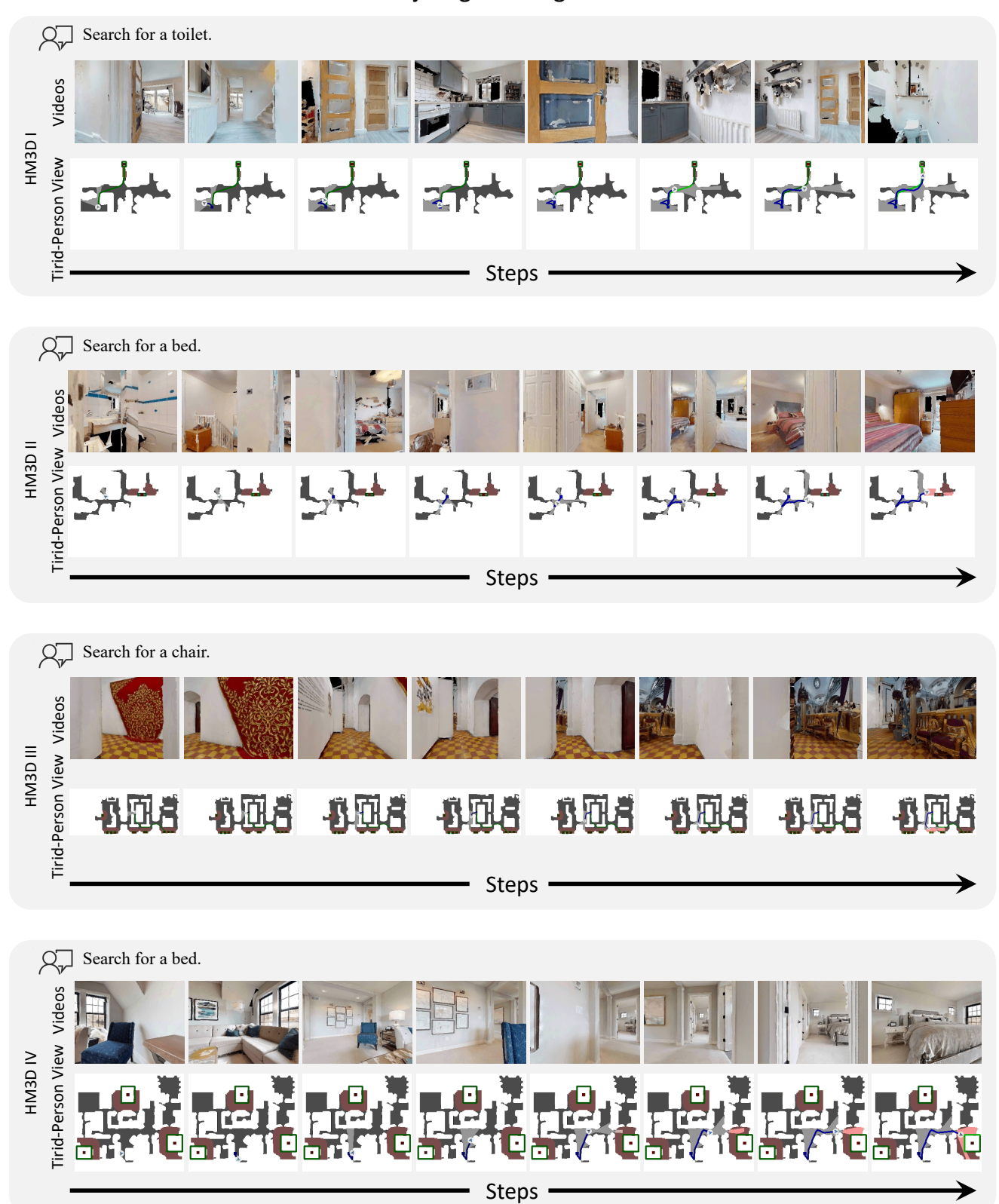


Figure 11. Visual results of HM3D ObjectNav.

Embodied Question Answering

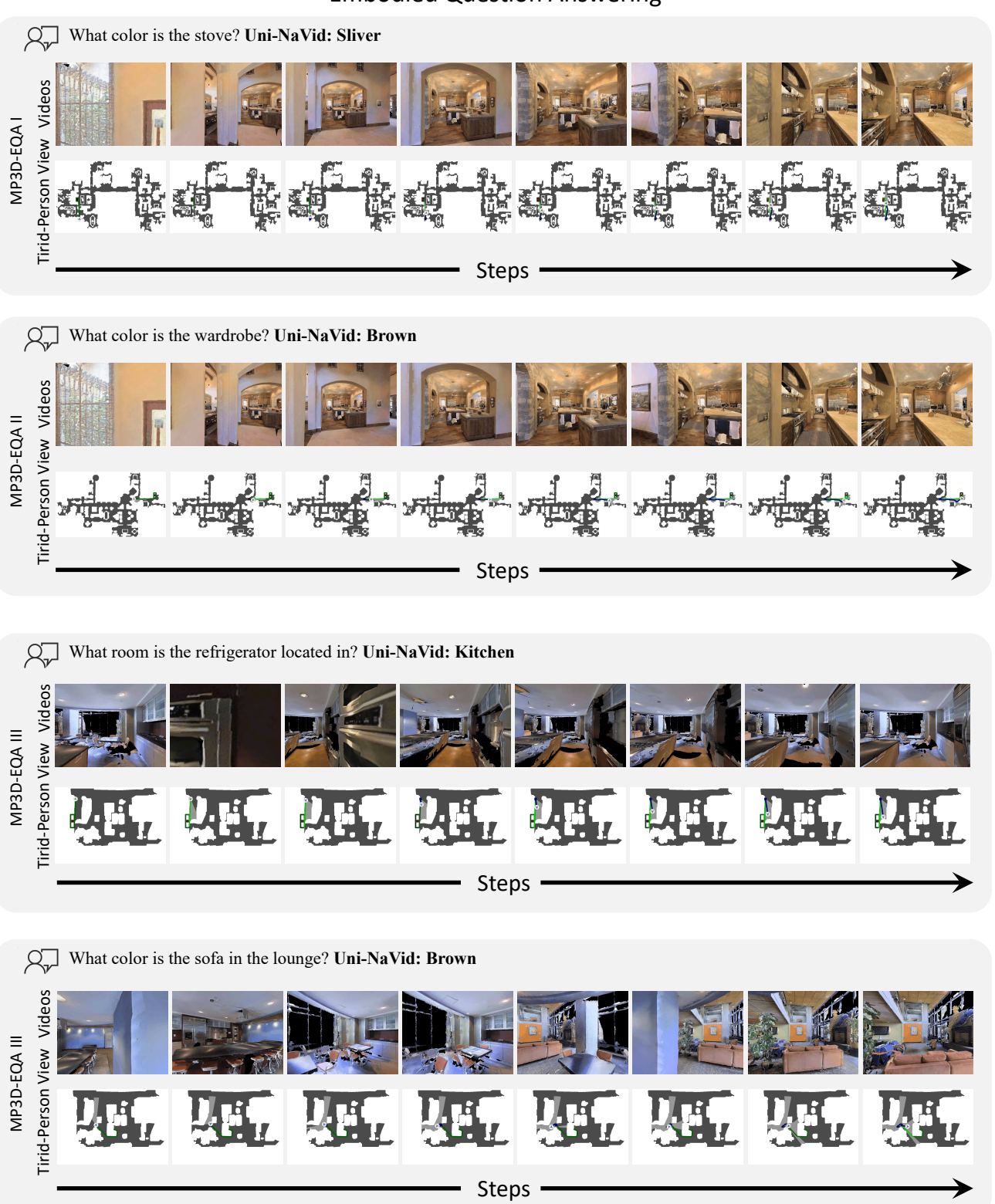


Figure 12. Visual results of MP3D-EQA.

Human Following

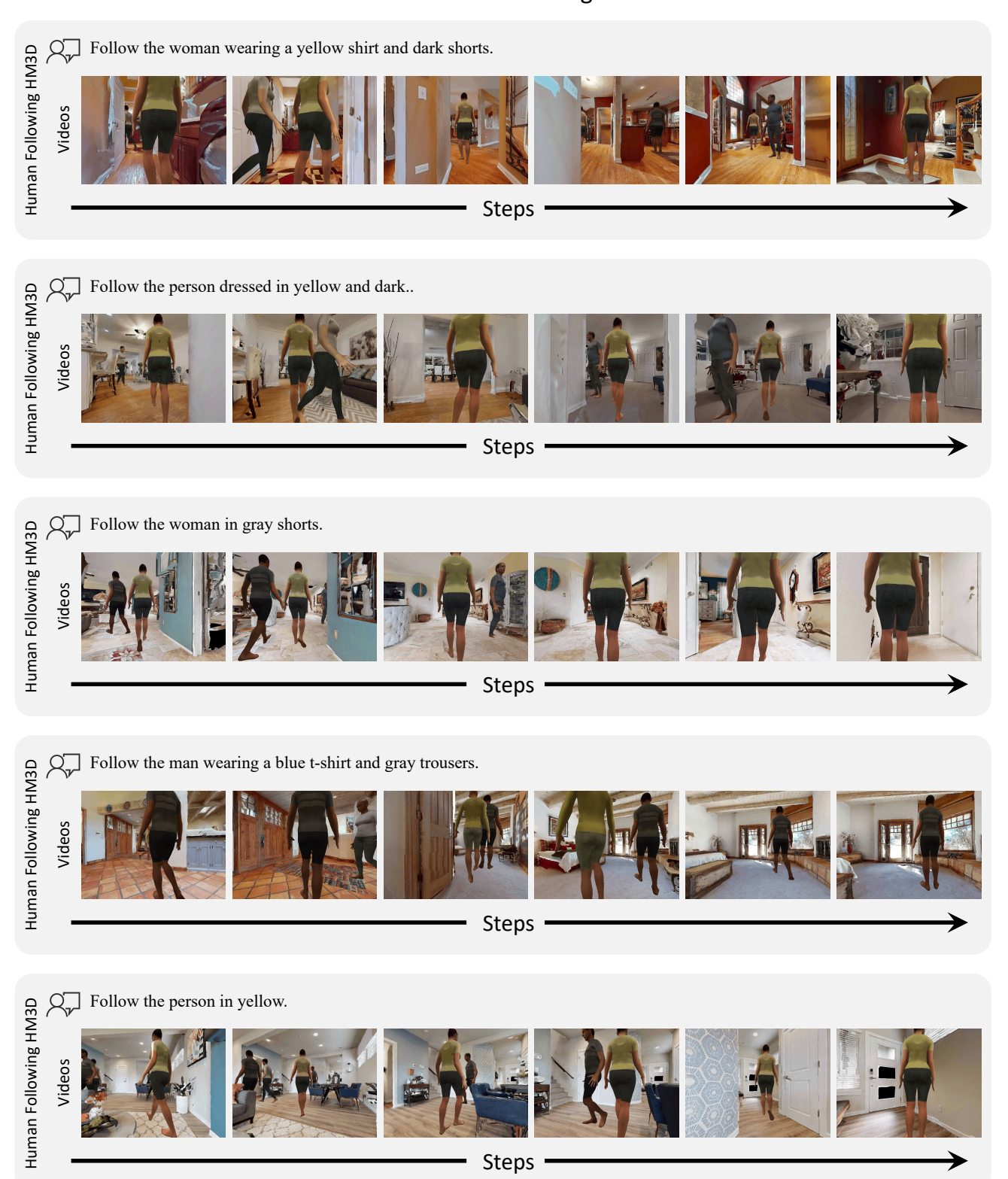


Figure 13. Visual results of HM3D Human following.